

Fig. 1. Computed tomography of the brain showing bilateral atrophy of the frontal and temporal lobes with pallidal calcification (Case 8).

FTLD-U and amyotrophic lateral sclerosis (ALS) [8,9]. Subsequent studies have demonstrated the concurrence of TDP-43, tau, and alpha-synuclein (aSyn) pathology in other neurodegenerative disorders including AD, Dementia with Lewy bodies (DLB), Guamanian ALS/parkinsonism–dementia complex (G-PDC) and argyrophilic grain disease (AGD) [10–14]. However, it remains unclear whether or not these pathological proteins coexisted within the same neuron. In addition, although the clinical symptoms of DNTC have been attributed to a partial mixture of AD and FTLD [1], the way in which these neuropathological changes contribute to the clinical symptoms is not fully understood at present. Especially because the symptoms of DNTC clinically closely mimic those of FTLD, it is important to observe the pathology of DNTC specifically for a comparison with FTLD.

In order to clarify the proteinopathy of DNTC in this study, 1) we performed detailed immunohistochemical analyses of 10 Japanese DNTC cases, using phosphorylation-dependent anti-TDP-43 antibodies and anti aSyn antibodies. 2) Furthermore, we investigated the colocalization or non-colocalization of these proteins in DNTC using the technique of double-label immunofluorescence staining. 3) In addition, we considered the correlation between the clinical symptoms and the neuropathological findings based on the immunohistochemical investigations mentioned.

2. Materials and methods

2.1. Materials

Ten autopsied DNTC cases were examined (2 male, 8 female). The age at death ranged from 56 to 79 years (average 67.0 years). The weights of the brains ranged from 850 to 1265 g (average 1050 g) (Table 1). In all cases except one (Case 9), there were temporal or frontotemporal lobar atrophy, widespread NFTs, a paucity of plaques and pronounced Fahr's-type calcification in the basal nuclei or cerebellum, consistent with the neuropathological criteria of DNTC [2]. Case 9 was previously diagnosed as DNTC despite a lack of atrophy

[15]. Detailed clinical data on some cases were previously reported elsewhere [1,16].

2.2. Methods

2.2.1. Tissue preparations

The brains were fixed with 10% buffered formalin and paraffin-embedded. Brain blocks of the frontal lobe, parietal lobe, temporal lobe, brainstem, and limbic region (including the amygdala, retro hippocampal formation, and parahippocampal gyrus), were cut into 5 μ m-thick slices in the coronal section. All sections were stained with hematoxylin and eosin, Klüver–Barrera's method and Gallyas–Braak method (GB).

2.2.2. Immunohistochemistry

Immunohistochemistry was carried out using the avidin–biotin peroxidase complex technique (Vectastain ABC Kit; Vector Laboratories, Burlingame, CA, USA). Immunohistochemical staining was performed using anti-phosphorylated aSyn (Wako, concentration 1:3000), anti-TDP-43 (Protein Tech, 1:2000), and anti-phosphorylated TDP-43 (pTDP) (pS409/410 and pS403/404 [17], 1:1000, respectively). Some specimens were stained with anti-paired helical filament tau mouse monoclonal antibody (AT8; Innogenetics, Zwijndrecht, Belgium, 1:100). The sections were finally mounted in a glycerol-based medium and then observed using a light microscope. The Lewy body type, and the degree and distribution of Lewy pathology, were assessed by pathologic assessment and diagnostic criteria for DLB [18]. Furthermore, we assessed the TDP-43 pathology following the study of Amador-Ortiz, C. et al. [10]. Cases having more severe pathology outside of the temporal lobe were considered to have “diffuse” TDP-43 immunoreactivity. Cases with involvement relatively confined to the limbic lobe were referred to as “limbic.” The TDP-43-positive structure was assessed using the following scheme: 0 = none, 1 = slight, 2 = mild, 3 = moderate, 4 = severe.

2.2.3. Double labeling immunofluorescence study

A double labeling immunofluorescence study was performed for pTDP-43 and phosphorylated tau, or for pTDP-43 and phosphorylated aSyn in Cases 2 and 8. The sections were incubated overnight at 4 °C in a cocktail of pS403/404 [17] and AT8 (Innogenetics, 1:100) or anti aSyn (Wako, 1:3000). After washing with PBS containing 0.3% Triton X-100 (Tx-PBS) for 30 min, the sections were incubated for 2 h at room temperature in a cocktail of fluorescein isothiocyanate-conjugated goat anti-mouse IgG (1:100; Millipore, Temecula, CA) and tetramethylrhodamine isothiocyanate-conjugated goat anti-rabbit IgG (1:100; Millipore). After washing, the sections were incubated in 0.1% Sudan Black B for 10 min at room temperature and washed with Tx-PBS for 30 min. The sections were coverslipped with Vectashield (Vector Laboratories) and observed with a confocal laser microscope (LSM5 PASCAL; Carl Zeiss Microimaging GmbH, Jena, Germany).

2.2.4. Relationship between histopathology and clinical features

The clinically characteristic symptoms were investigated and summarized from the clinical charts and previous reports [1,15,16]. From this information, we assessed the neuropsychiatric symptoms of the 10 cases referring to the evaluation items of the Neuropsychiatric Inventory Questionnaire (NPI-Q) [19], in addition to cognitive and functional decline and verbal disturbance. We extracted three items from NPI-Q which are supposed to be marked, especially in FTLD cases: a) apathy or indifference, b) disinhibition (impulsiveness), and c) motor disturbance (pacing, compulsive behaviors). We investigated the statistical relationships between the scores of these characteristic items and the severity score of pathological findings. Statistical analyses were performed using Spearman's correlation coefficient method with $p < 0.05$ considered statistically significant.

Table 1
Clinical features and neuropathological findings of 10 DNCT cases.

Case		1	2	3	4	5	6	7	8	9	10		
Clinical diagnosis		PSD	AD	PSD	PiD	NANPD	AD+BD	NANPD	PiD	SPs	Sc		
General information	Background	Sex	F	F	F	M	F	F	M	F	F	F	
		Age at onset (years old)	46	49	51	52	56	56	59	64	65	NA	
		Age at death (Duration years)	68(22)	57(8)	59(8)	56(4)	64(8)	79(17)	73(4)	72(8)	70(5)	72	
		Cause of death	Pn	Inf	Inf	Pn	Pn	Inf	RnF	RnF	Pn	RnF	
		Heredity	No	No	No	No	No	CVD, Sc	No	No	No	No	
		Past history	No	No	Tb	No	No	Con	No	Men	No	SAH	
	Brain	Weight (g)	850	1050	1140	1260	1000	920	1030	970	1265	1015	
	Atrophy region	FL, TL	FL, TL	TL	FL, TL	TL	FL, TL	FL, TL	FL, TL	None	TL		
Clinical findings	Memory disturbances (None, ±, +, ++)		++	+	+	±	+	+	+	±	None		
	Verbal disturbances (None, +)		None	+	+	+	+	+	+	+	None		
	Neurological symptoms		Pa, Ps	None	None	Pa	None	Dev	Pa, Ps	None	None		
	†Personality changes	Three extracted items of NPI-Q score	Apathy	12	8	12	12	2	0	8	0	8	12
			Disinhibition	12	12	0	0	0	0	12	12	12	0
			Motor disturbance	0	0	12	8	0	0	12	8	0	8
			Total score	24	20	24	20	2	0	32	20	20	20
‡TDP-43 pathology	TDP-43 score	Distribution pattern		Limbic	Diffuse	Diffuse	Diffuse	Diffuse	Limbic	Diffuse	Diffuse	NA	Diffuse
		†††FTLD-TDP subtype		NA	2	2	2	2	NA	3	2	NA	2
		FC and TC	PC	0	1	0	0	0	0	3	0	0	1
			FC	NA	0	0	0	0	0	0	NA	0	0
			TC	0	2	1	3	2	0	4	2	0	4
			Total score	0	2	1	3	2	0	4	2	0	4
		LR	AMYG	4	NA	1	1	1	1	4	1	0	2
			HIP	1	2	1	0	0	1	1	2	0	1
			DG	0	1	0	0	0	0	0	0	0	0
			EC	0	3	1	3	1	0	2	2	0	2
			Total score	5	6	3	4	2	2	7	5	0	5
		FC, TC and LR total score		5	8	4	7	4	2	11	7	0	9
		Brain stem	BN	0	0	0	0	1	0	0	0	0	1
SN	NA		NA	1	NA	1	NA	1	1	NA	1		
††††Lewy pathology	aSyn score	Distribution pattern		Limbic	NA	Limbic	Diffuse neocortical	Limbic	Diffuse neocortical	Diffuse neocortical	Diffuse neocortical	NA	Diffuse neocortical
		LR	HIP	2	0	3	4	3	4	4	4	0	4
			DG	0	0	0	1	0	3	1	0	0	0
			Brain stem	NA	NA	2	NA	2	NA	3	2	NA	2
Tau pathology	NFT (Braak Stage)		VI	VI	VI	VI	VI	VI	VI	VI	VI		

AD: Alzheimer's disease, AMYG: amygdala, aSyn: alpha-synuclein, BD: Binswanger's Disease, BN: basal nuclei, Con: convulsion, CVD: cerebrovascular disease, Dev: tongue deviation on protrusion, DG: hippocampal dentate gyrus, EC: entorhinal cortex, F: female, FC: frontal cortex, FL: frontal lobe, HIP: hippocampus, Inf: infection, LR: limbic region, M: male, Men: meningitis, NA: not available, NANPD: non-Alzheimer non-Pick dementia, NFT: neurofibrillary tangles, NPI-Q: Neuropsychiatric Inventory Questionnaire, Pa: parkinsonism, PC: parietal cortex, PiD: Pick disease, Pn: pneumonia, Ps: pyramidal sign, PSD: presenile dementia, RnF: renal failure, SAH: subdural hemorrhage, Sc: schizophrenia, SN: substantia nigra, SPs: senile psychosis, Tb: pulmonary tuberculosis, TC: temporal cortex, TDP-43: TAR DNA-binding protein of 43 kDa, TL: temporal lobe.

†Personality changes were assessed according to the Neuropsychiatric Inventory Questionnaire (score 0–12).

††The distribution pattern of TDP-43 was assessed following the study of Amador-Ortiz et al. [10]. The TDP-43-positive inclusions were assessed using the following scheme: 0: none, 1: slight, 2: mild, 3: moderate, and 4: severe.

†††FTLD-TDP subtype was assessed using the classification of Sampathu et al. [24].

††††The Lewy body type, and the degree (alpha-synuclein score (0–4)) and distribution of Lewy pathology, were assessed by pathologic assessment and diagnostic criteria for DLB (McKeith et al. [18]).

Statistical analyses were performed using Spearman's correlation coefficient method with $p < 0.05$ considered statistically significant.

* $p > 0.05$, ** $p < 0.05$, *** $p > 0.05$.

3. Results

3.1. Pathological findings

3.1.1. Tau pathology

In all cases, GB stain showed widespread and abundant NFTs throughout the neocortex and limbic system, especially the temporal cortex, hippocampus, and amygdala. The distribution pattern of NFTs indicated that all cases were classified as stages V or VI based on Braak and Braak staging [20].

3.1.2. The aSyn pathology

Alpha-Syn positive inclusions and neurites were observed in 8 cases (Cases 1, 3, 4, 5, 6, 7, 8, 10 in Table 1). The distribution of aSyn

pathology was confined to the limbic region in 3 (Cases 1, 3, 5) of 8 cases, and extended to the neocortex in the other 5 cases. The former 3 cases were identified as the limbic type, and the latter 5 cases as the diffuse neocortical type, according to the classification of DLB by the study of McKeith et al. [18] (Table 1) (Fig. 2A). In the limbic region, aSyn-positive structures were present in dentate granule cells of the hippocampus in 3 cases (Cases 4, 6, 7) (Fig. 2B), in pyramidal neurons of CA2 and CA3 areas in 6 cases (Cases 3, 4, 6, 7, 8, 10) (Fig. 2C), and in the deep layer of the parahippocampal cortex in all 8 cases (Fig. 2D–F).

3.1.3. TDP-43 pathology

The pTDP-43 immunopositive structures were observed in 9 of 10 cases (Table 1). Regarding the distribution of pTDP-43 pathology, 2

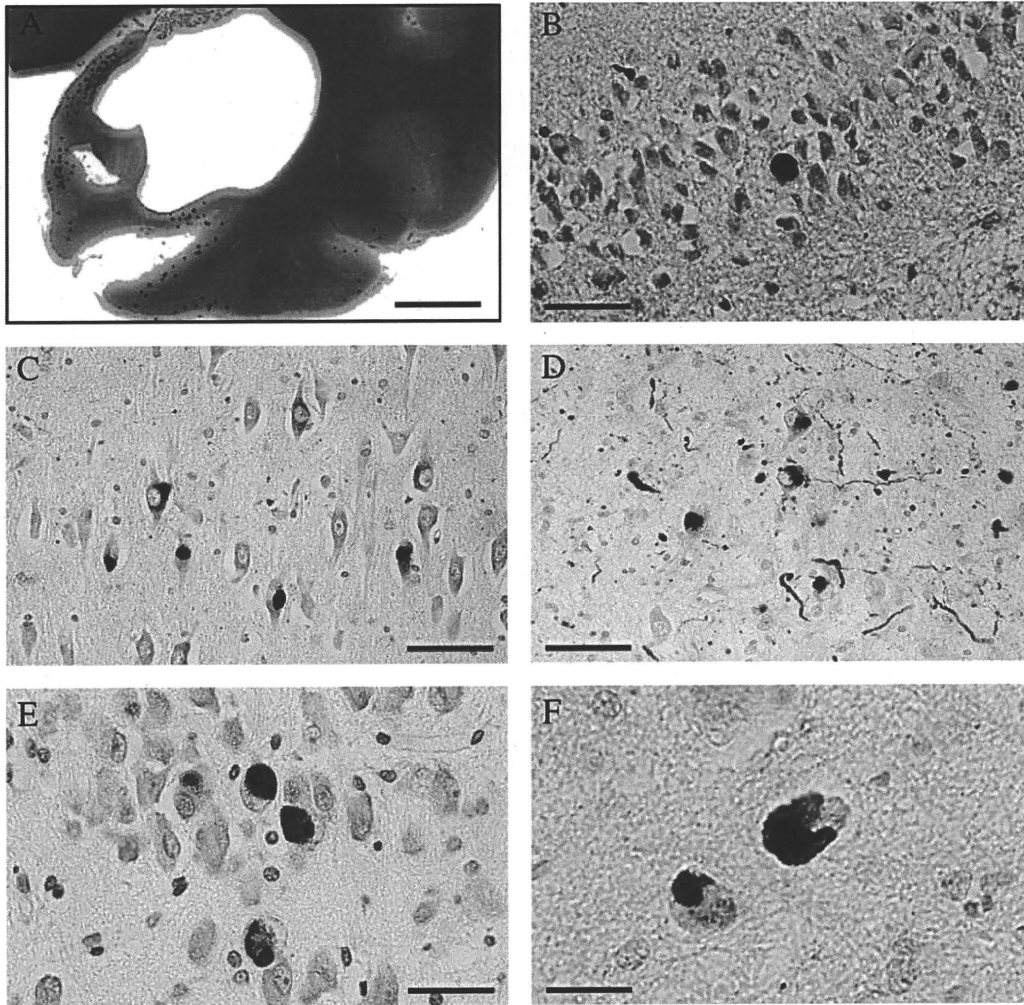


Fig. 2. A. Appearance of Lewy bodies and Lewy neurites in Case 8 (alpha-synuclein immunostaining: one dot indicates one Lewy body). B. Lewy bodies were observed in the dentate granule cell layer in the hippocampus (Case 6). C. Lewy bodies and neurites were observed in CA3 of Case 4. Scale bar = 50 μ m. Lewy bodies were observed in the deep layer of the parahippocampal cortex (D (Case 7), E (Case 3), and F (Case 5)). Scale bar: A, 5 mm; B, C, 50 μ m; D, E, and F, 20 μ m.

of 9 cases showed pTDP-43 pathology confined to the limbic region, while the other 7 cases showed more widespread pTDP-43 pathology to the temporal neocortex. Of the 7 cases with pTDP-43 pathology in the neocortex, 6 cases (Cases 2, 3, 4, 5, 8, 10) showed predominant neuronal cytoplasmic inclusions (NCIs) with a few dystrophic neurites (DNs) (Fig. 3A–D), while Case 7 showed abundant NCIs and DNAs (Fig. 3H–J). Glial cytoplasmic inclusions (GCIs) were also observed in all 9 cases (Fig. 3E–G). NCIs in the dentate granular cells were found only in one (Case 2) of 9 cases. No neuronal intranuclear inclusions were seen in any of the cases.

Neuronal cytoplasmic granular structures positive for pTDP-43 but negative for a commercial anti-TDP-43 antibody were observed in 6 cases (Cases 2, 4, 5, 7, 8, 10) (Fig. 3K, L). Four (Cases 2, 7, 8, 10) of these showed both pTDP-43 positive cytoplasmic granules and NCIs/GCIs, while 2 cases (Cases 4, 5) showed only granules.

3.1.4. Colocalization of TDP-43 and aSyn or Tau

In double labeling immunofluorescence of the sections of the hippocampal region, a scarce colocalization of pTDP-43 and phosphorylated aSyn or a scarce colocalization of pTDP-43 and phosphorylated tau was observed in neuronal cytoplasm with very low frequency. However, we did see partial colocalization of aSyn and pTDP-43 in some neuronal cytoplasmic inclusions in the deep layer of the entorhinal cortex, and partial colocalization of tau and pTDP-43

in some neuronal cytoplasmic inclusions and the dentate gyrus of the hippocampus. Upon double-immunofluorescent labeling of cytoplasmic inclusions, pTDP-43 was scarcely superimposed with aSyn or tau (Fig. 4).

3.2. Clinical features

The clinical features of each patient are summarized in Table 1. Basically, the main symptoms comprised memory disturbances, verbal disturbances, or personality and behavioral changes in all cases. The degree of memory disturbance was moderate to severe in 7 cases (Cases 1, 2, 3, 5, 6, 7, 8). Verbal disturbances were found in 8 cases. Of these, 3 cases (Cases 5, 7, 8) showed verbal symptoms similar to primary progressive non-fluent aphasia, while one case (Case 2) showed semantic dementia-like symptoms. Regarding neurological symptoms, pyramidal signs including Babinski's sign were observed in 2 cases (Cases 1, 7), and parkinsonism in 3 cases (Cases 1, 4, 7).

Neuropsychiatric symptoms, including personality and behavioral changes, were assessed according to NPI-Q. Regarding personality changes, the symptoms of apathy or indifference were severe in 4 cases (Cases 1, 3, 4, 10). The symptoms of disinhibition characterized by morbid impulsions and 'going my way' behavior (i.e., lack of consideration for the feelings of others) were severe in 5 cases (Cases 1, 2,

7, 8, 9). The symptoms of motor disturbances, including pacing and compulsive behavior, were severe in 2 cases (Cases 3, 7).

3.3. Clinical features and pathology

We examined the relationship between the clinical features and aSyn pathology or TDP-43 pathology. Three cases (Cases 4, 6, 7) showed a higher aSyn score with aSyn-positive inclusions in dentate granular cells in the hippocampus and were identified as the diffuse neocortical type. Such cases tended to have neurological symptoms, including rigidity and akinesia (Cases 4, 7 in Table 1).

Two cases with spontaneous features of parkinsonism and progressive cognitive decline (Cases 4, 7, in Table 1) satisfied the clinical diagnostic criteria of possible DLB [18], and were thought to be categorized as the diffuse neocortical type. Among five cases (Cases 3, 5, 7, 8, 10) with brainstem synuclein pathology, only one case (Case 7) clinically showed parkinsonism.

From the viewpoint of clinical characteristics and TDP-43 pathology, cases with frequent pTDP-43-positive NCI/GCI in the hippocampus and amygdala tended to show higher scores of certain items in the NPI-Q (Cases 1, 7 in Table 1).

There were no significant correlations between the score of limbic TDP pathology and the score of each extracted item (apathy, disinhibition, and motor disturbances) of NPI-Q focused on three main

clinical feature-associated frontotemporal symptoms (Spearman's correlation coefficient; 0.190, 0.459, and 0.394, respectively, all with p -value > 0.05). However, there was a significant correlation between the score of limbic TDP pathology and the combined score of these three extracted items (Spearman's correlation coefficient 0.573, p -value < 0.05). In contrast, there was no correlation between the sum of the scores of those three extracted items of NPI-Q and the severity score of frontotemporal TDP pathology (Spearman's correlation coefficient 0.200, p -value > 0.05), nor the severity score of frontotemporal and limbic total TDP pathology (Spearman's correlation coefficient 0.441, p -value > 0.05).

4. Discussion

In this study, we found high frequencies of cerebral accumulation of TDP-43 (90%) and of aSyn (80%) in DNTC. The accumulation of both abnormal proteins was observed in the limbic region most frequently. The immunoreactivity of TDP-43 was observed to further extend to the neocortex, in almost all cases presenting TDP-43 pathology. In addition, a significant correlation between the sum of the scores of certain question items of the NPI-Q and the score of the limbic TDP-43 pathology suggests that the abnormality of TDP-43 plays an important role in the pathological process and FTL-like symptoms of DNTC.

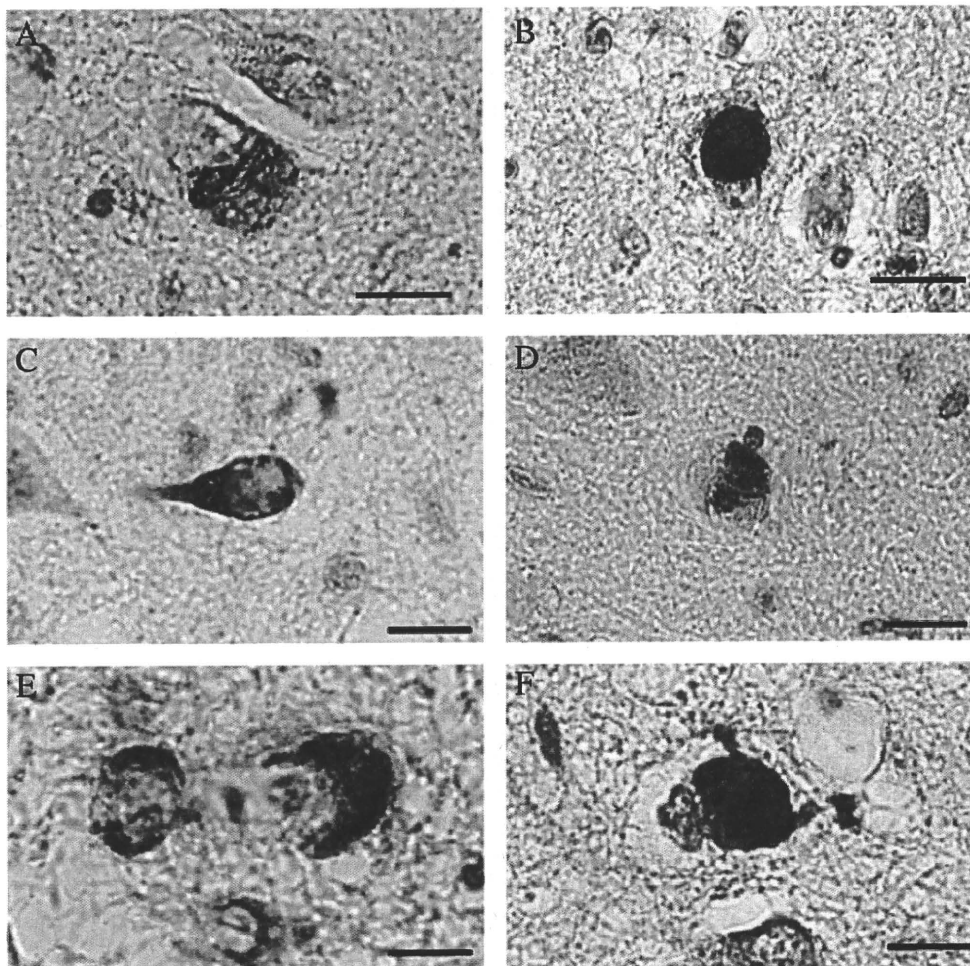


Fig. 3. NCIs were seen in the CA2 areas of Case 8 (A) and Case 1 (B) (anti-pTDP-43). NCIs were seen in the CA2 areas of Case 7 (C) and Case 8 (D) (anti-TDP-43). E. GCI-like structures were observed in the deep layer of the parahippocampal cortex in Case 7 (anti-pTDP). GCI was seen in the CA2 area (F) and CA3 area (G) of Case 2 (anti-pTDP). GCI-like structures and DNs were observed in the deep layer of the middle temporal gyrus (H), in the amygdala (I), and in the deep layer of the parahippocampal cortex (J) of Case 7 (anti-pTDP). Granular cytoplasmic pTDP-positive structures were observed in the CA2 area of Case 5 (K), and in the CA1 area of Case 4 (L) (anti-pTDP). Scale bar: A, C, E, and F, 10 μ m; B, D, H, I, J, K, and L, 20 μ m; G, 50 μ m.

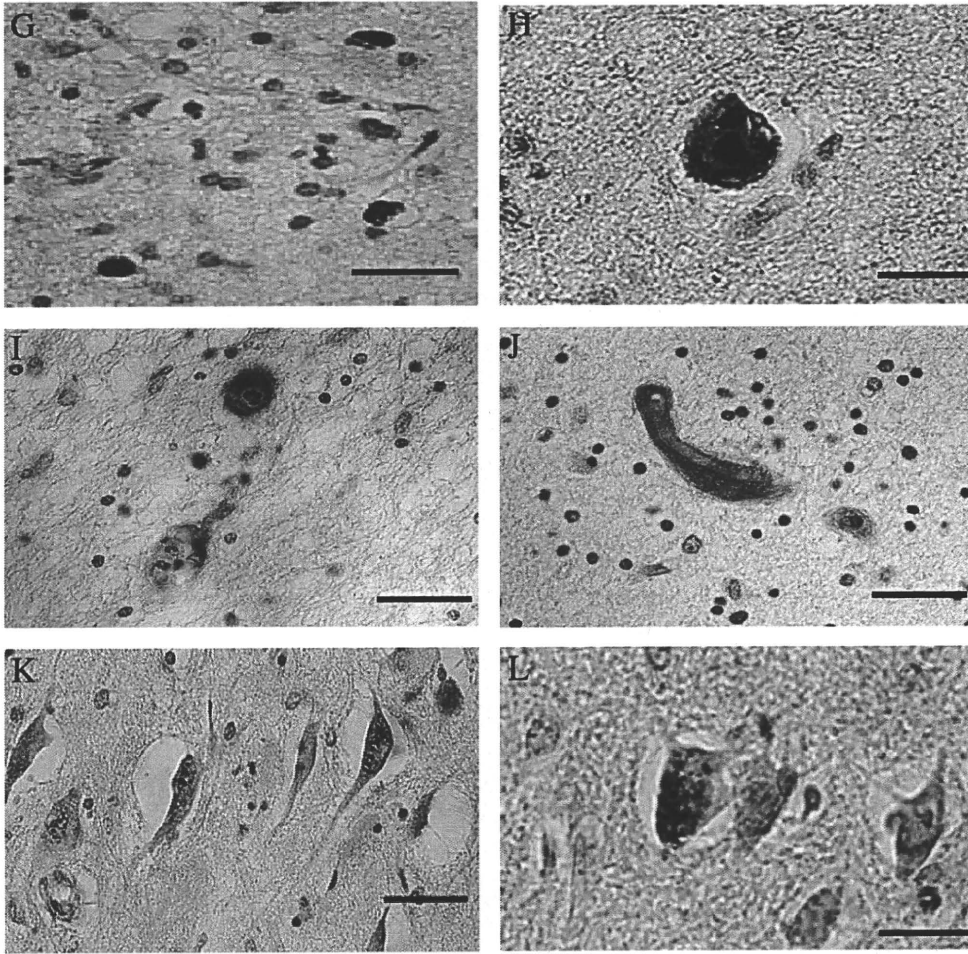


Fig. 3 (continued).

4.1. Alpha-Syn pathology in DNTC

The area of limbic region seemed to be the most vulnerable for aSyn pathology as well as tau pathology in DNTC (Table 1). These observations are consistent with the previous reports [21,22].

4.2. TDP-43 pathology in DNTC

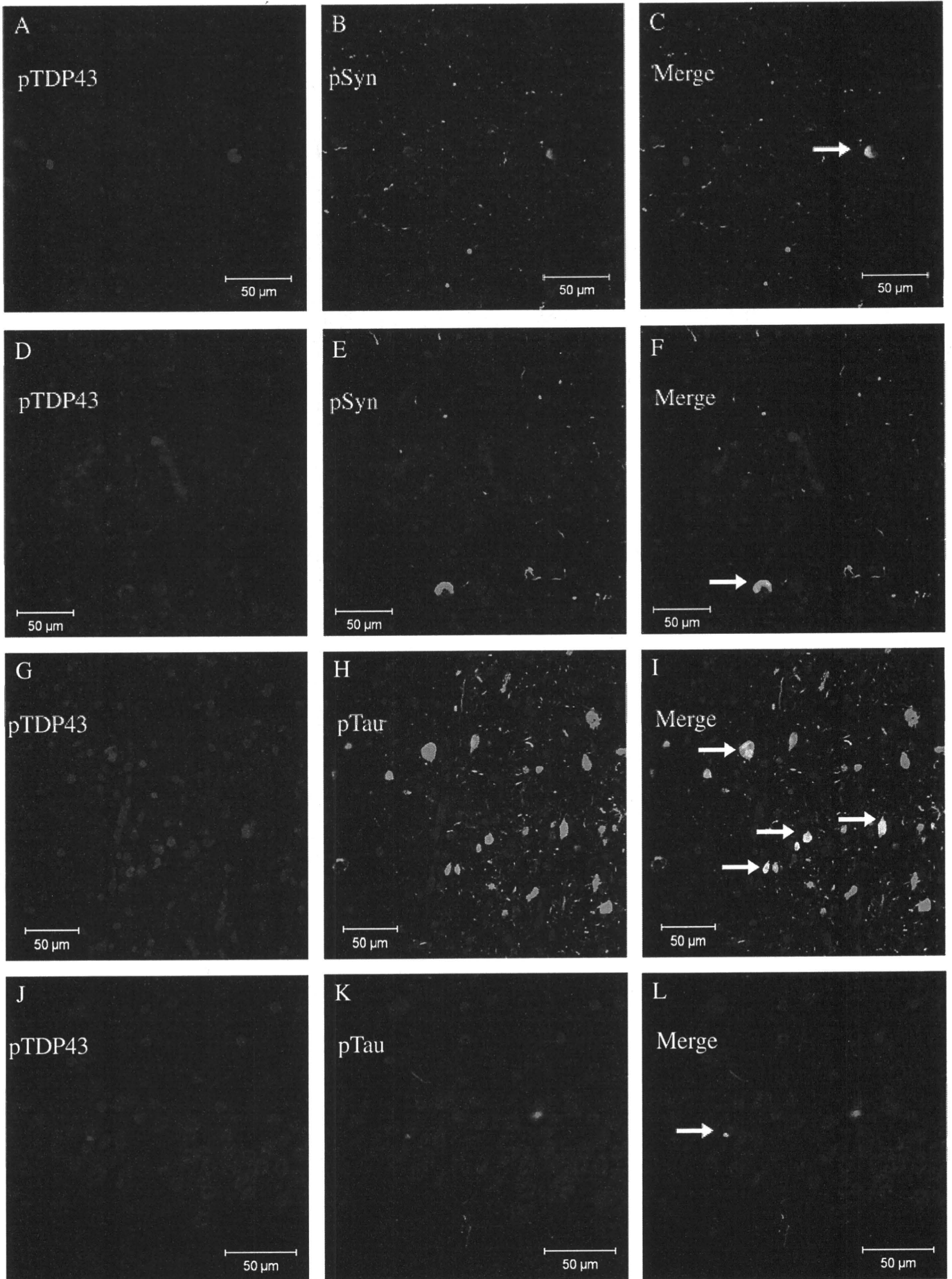
We demonstrated a high frequency of TDP-43 pathology in 9 out of 10 DNTC cases (90%). Among the 9 cases having pTDP-43 pathology, 2 cases (Cases 1, 6) (22%) were identified as the 'limbic type,' while the other 7 cases (Cases 2, 3, 4, 5, 7, 8, 10) (77%) were "diffuse type," according to the classification by the study of Amador-Ortiz et al. [10]. The vulnerability of the limbic region to pTDP-43 accumulation found in our DNTC series was consistent with the previous reports of AD, DLB and AGD [10,11,13,14,23].

We mainly observed the pathology of DNTC for the purpose of comparison with FTLD. Recently, the TDP-43 pathology in FTLD has been classified into 4 subtypes according to the cortical TDP-43 pathology [24–26]. In the present study, 6 out of 7 cases (86%) with cortical TDP-43 pathology showed many NCIs/GCIs and sparse DNs,

similar to the FTLD with ubiquitin-positive, tau-negative, TDP-43 positive neuronal cytoplasmic inclusions (FTLD-TDP), Type 2, using current terminology [27]. Only one case (Case 7) showed many NCI/GCIs and DNs, similarly to FTLD-TDP, Type 3. These findings of TDP-43 pathology in DNTC differ from those of AD and DLB cases, which almost all present Type 3 pathology [13,28,29].

In this point, the question arises as to whether this high frequency of TDP-43 pathology in DNTC cases represents a concurrent primary pathological process of FTLD-TDP or a secondary change occurring in susceptible neuronal populations. Although the high frequency of GCIs in DNTC is similar to the pathology of FTLD-TDP, Type 2, a simple coincidence of FTLD-TDP and DNTC seems unlikely based on our findings as follows. First, the main TDP-43 pathology in DNTC is similar to Type 2, but the frequency of TDP-43 positive NCIs in the dentate gyrus was low (one out of 9 cases; 11%) in our DNTC cases with TDP-43 immunoreactivity in comparison with those (about 80%) in FTLD-TDP, Type 2 [25,30]. Second, there are previous reports that 25–40% of FTLD-TDP cases with Type 2 pathology tend to be associated with clinical features of motor neuron disease [25,31]. In contrast, there was no case with Type 2-like pathology showing clinical features of motor neuron disease in our DNTC series.

Fig. 4. Double labeling immunofluorescence in Case 8 (A–F) demonstrates that most alpha-synuclein positive inclusions (green fluorescence in B, E) and pTDP-43 positive inclusions (red fluorescence in A, D) in the CA3 area of the hippocampus are independent (F), while there is partial colocalization of alpha-synuclein and pTDP-43 in some neuronal cytoplasmic inclusions in the deep layer of the entorhinal cortex (arrows in C). Double labeling immunofluorescence in Case 2 (G–L) demonstrates that most tau-positive neuropil threads (green fluorescence in H, K) and pTDP-43 positive inclusions (red fluorescence in G, J) in the entorhinal cortex are independent (L), while there is partial colocalization of tau and pTDP-43 in some neuronal cytoplasmic inclusions and the dentate gyrus of the hippocampus (arrows in I). Scale bar: A–L, 50 μ m.



Therefore, it may be possible to speculate that TDP-43 pathology in DNTC has different characteristics from that of FTLD-TDP.

There arises another query concerning the possibility that the results in this study were driven by cross-reactive phospho-epitopes because the antibodies used for tau, aSyn and TDP-43 in this study were all phosphorylation-specific. Although there is some evidence of cross-reactivity with phosphorylated aSyn and phosphorylated tau [32], the anti-phosphorylated aSyn antibody used in this study did not immunostain NFT in AD brains, suggesting that it does not have cross-reactivity with phosphorylated tau.

Since the posttranslational modification is known to be a common motif in pathological protein accumulation in many neurodegenerative disorders and also this process can involve phosphorylation [33–36], the phosphorylation-dependent antibodies could mostly detect the pathological TDP-43 inclusions [13,17,37]. These mechanisms of phosphorylation might proceed in the pathologies of tau [34] or synuclein [38].

We found a scarce colocalization of pTDP-43 and tau and/or aSyn in some neuronal cytoplasmic inclusions in this study. Such a partial colocalization of tau (grain, or NFT), aSyn, and TDP-43 is consistent with that previously reported in AD, DLB, Pick's Disease, AGD, G-PDC and corticobasal degenerations to a varying degree [10–14,23]. As for the double-labeled cytoplasmic inclusions within the neuron, some reports [11,14] indicated that the TDP-43 was hardly superimposed with tau or observed only in a part of tau-positive cytoplasmic inclusions in AD or AGD based on double confocal microscopic observation. Also in this study, pTDP-43 scarcely coexisted with tau in neuronal cytoplasmic inclusions. These facts suggested that the pathway of appearance of the TDP-43 pathology might be different from that of the tau pathology but could relate closely in some way to tau proteinopathy of neurodegenerative diseases including DNTC.

It is possible that these findings were resulted from a non-specific vulnerability of the limbic region against these proteinopathies. However, there may be common factors or mechanisms that affect the conformation or modification of those proteins, leading to their intracellular accumulation. Especially, it was interesting to note that the results of the present study further supported the previous report that indicated similarity between DNTC and G-PDC [39]. Both disorders are assumed to be some type of endemic disease, and show frontotemporal atrophy and accumulation of tau, aSyn and TDP-43 without Amyloid β deposition. These findings could offer a hint toward understanding of the pathogenesis of these disorders.

4.3. Clinical features and pathology in DNTC

The phosphorylated aSyn pathology was observed in the brain stem of 5 cases of DNTC, but only one of these 5 cases had presented parkinsonism clinically. There seems to be a discrepancy between the presentation of parkinsonism and the pathological findings of phosphorylated aSyn appearance in DNTC.

There are some reports referring to an association between a specific clinical symptom and an underlying pathology in diverse degenerative disorders [40–43]. In our DNTC cases, the limbic region seemed to be the most vulnerable to abnormal accumulation of tau, aSyn and TDP-43. Thus, there is a possibility that not only accumulation of tau but also accumulation of aSyn and TDP-43 in the limbic region may be associated with early onset cognitive decline in DNTC. Indeed, in AD, concurrent TDP-43 pathology was reported to be associated with more severe cognitive decline [40].

In this study, we found a comprehensive association between pTDP-43 pathology and the frontotemporal symptoms (apathy, disinhibition, motor disturbances) in DNTC. Clinically, DNTC was diagnosed as FTLD because these three symptoms are representative and appear simultaneously to various degrees, so the integration of these three symptoms was very important for clinical assessment. Velakoulis, D. et al. recently reported that abnormalities in TDP-43

nuclear expression in the hippocampus were identified in patients with late-onset psychosis and a positive family history [44]. These findings suggest that abnormality of TDP-43 may be involved in the psychiatric symptoms of DNTC.

Meanwhile, there were some reports of DNTC without sufficient clinical or pathological assessment [4,45,46]. Cases of Fahr's syndrome with neuropsychological deficits and neuropsychiatric features have also been reported based on radiological findings [3,47,48]. More investigation will be needed to identify Fahr's syndrome as having the same background pathology of DNTC.

The association between basal ganglia calcification and psychotic symptoms has also been reported [49], but it remains unknown how the pathogenesis of calcification phenomenon concerns the psychosis. In the clinical setting, DNTC might pass unnoticed because it presents various clinical symptoms during the clinical course. Further studies on such cases from clinical, radiological and pathological standpoints might help elucidate the pathogenesis of DNTC.

5. Further assignment

We declare that there are some limitations of this study. Firstly, all the tissue samples were embedded in paraffin, so we could not perform molecular investigations including the Western Blotting test. Secondly, there were only a couple of sets of neuroimaging data of low resolution computed tomography available to this study, so we could not evaluate the association among the neuroimaging, neuropathology, and clinical symptoms. To address these issues, we are currently trying to upgrade the method for preserving tissue samples, and will acquire more neuroimaging data for a future prospective study.

References

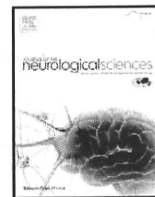
- [1] Shibayama H, Kobayashi H, Nakagawa M, Yamada K, Iwata H, Iwai K, et al. Non-Alzheimer non-Pick dementia with Fahr's syndrome. *Clin Neuropathol* 1992;11: 237–50.
- [2] Kosaka K. Diffuse neurofibrillary tangles with calcification: a new presenile dementia. *J Neurol Neurosurg Psychiatry* 1994;57:594–6.
- [3] Modrego PJ, Mojonero J, Serrano M, Fayed N. Fahr's syndrome presenting with pure and progressive presenile dementia. *Neurol Sci* 2005;26:367–9.
- [4] Nanda S, Bhatt SP, Pamula J, Woodruff WW, Fowler M, Miller D. Diffuse neurofibrillary tangles with calcification (DNTC): Kosaka-Shibayama disease in America. *Am J Alzheimers Dis Other Demen* 2007;22:535–7.
- [5] Baker M, Mackenzie IR, Pickering-Brown SM, Gass J, Rademakers R, Lindholm C, et al. Mutations in progranulin cause tau-negative frontotemporal dementia linked to chromosome 17. *Nature* 2006;442:916–9.
- [6] Cruts M, Gijssels I, van der Zee J, Engelborghs S, Wils H, Pirici D, et al. Null mutations in progranulin cause ubiquitin-positive frontotemporal dementia linked to chromosome 17q21. *Nature* 2006;442:920–4.
- [7] Gass J, Cannon A, Mackenzie IR, Boeve B, Baker M, Adamson J, et al. Mutations in progranulin are a major cause of ubiquitin-positive frontotemporal lobar degeneration. *Hum Mol Genet* 2006;15:2988–3001.
- [8] Arai T, Hasegawa M, Akiyama H, Ikeda K, Nonaka T, Mori H, et al. TDP-43 is a component of ubiquitin-positive tau-negative inclusions in frontotemporal lobar degeneration and amyotrophic lateral sclerosis. *Biochem Biophys Res Commun* 2006;351:602–11.
- [9] Neumann M, Sampathu DM, Kwong LK, Truax AC, Micsenyi MC, Chou TT, et al. Ubiquitinated TDP-43 in frontotemporal lobar degeneration and amyotrophic lateral sclerosis. *Science* 2006;314:130–3.
- [10] Amador-Ortiz C, Lin WL, Ahmed Z, Personett D, Davies P, Duara R, et al. TDP-43 immunoreactivity in hippocampal sclerosis and Alzheimer's disease. *Ann Neurol* 2007;61:435–45.
- [11] Higashi S, Iseki E, Yamamoto R, Minegishi M, Hino H, Fujisawa K, et al. Concurrence of TDP-43, tau and alpha-synuclein pathology in brains of Alzheimer's disease and dementia with Lewy bodies. *Brain Res* 2007;1184:284–94.
- [12] Hasegawa M, Arai T, Akiyama H, Nonaka T, Mori H, Hashimoto T, et al. TDP-43 is deposited in the Guam parkinsonism–dementia complex brains. *Brain* 2007;130: 1386–94.
- [13] Arai T, Mackenzie IR, Hasegawa M, Nonaka T, Niizato K, Tsuchiya K, et al. Phosphorylated TDP-43 in Alzheimer's disease and dementia with Lewy bodies. *Acta Neuropathol* 2009;117:125–36.
- [14] Fujishiro H, Uchikado H, Arai T, Hasegawa M, Akiyama H, Yokota O, et al. Accumulation of phosphorylated TDP-43 in brains of patients with argyrophilic grain disease. *Acta Neuropathol* 2009;117:151–8.
- [15] Arai T, Kuroki N, Nizato K, Kase K, Iritani S, Ikeda K. An autopsy case of "diffuse neurofibrillary tangles with calcification", multiple infarctions and hyaline arteriosclerosis. *No To Shinkei* 1996;48:69–76.

- [16] Shibayama H, Hoshino T, Kobayashi H, Iwase S, Takenouchi Y. An autopsy case of atypical senile dementia with atrophy of the temporal lobes—a clinical and histopathological report. *Folia Psychiatr Neurol Jpn* 1978;32:285–98.
- [17] Hasegawa M, Arai T, Nonaka T, Kametani F, Yoshida M, Hashizume Y, et al. Phosphorylated TDP-43 in frontotemporal lobar degeneration and amyotrophic lateral sclerosis. *Ann Neurol* 2008;64:60–70.
- [18] McKeith IG, Dickson DW, Lowe J, Emre M, O'Brien JT, Feldman H, et al. Diagnosis and management of dementia with Lewy bodies: third report of the DLB Consortium. *Neurology* 2005;65:1863–72.
- [19] Kaufer DI, Cummings JL, Ketchel P, Smith V, MacMillan A, Shelley T, et al. Validation of the NPI-Q, a brief clinical form of the neuropsychiatric inventory. *J Neuropsychiatry Clin Neurosci* 2000;12:233–9.
- [20] Braak H, Braak E. Neuropathological staging of Alzheimer-related changes. *Acta Neuropathol* 1991;82:239–59.
- [21] Yokota O, Terada S, Ishizu H, Tsuchiya K, Kitamura Y, Ikeda K, et al. NACP/alpha-synuclein immunoreactivity in diffuse neurofibrillary tangles with calcification (DNFC). *Acta Neuropathol* 2002;104:333–41.
- [22] Hishikawa N, Hashizume Y, Ujihira N, Okada Y, Yoshida M, Sobue G. Alpha-synuclein-positive structures in association with diffuse neurofibrillary tangles with calcification. *Neuropathol Appl Neurobiol* 2003;29:280–7.
- [23] Hu WT, Josephs KA, Knopman DS, Boeve BF, Dickson DW, Petersen RC, et al. Temporal lobar predominance of TDP-43 neuronal cytoplasmic inclusions in Alzheimer disease. *Acta Neuropathol* 2008;116:215–20.
- [24] Sampathu DM, Neumann M, Kwong LK, Chou TT, Micsenyi M, Truax A, et al. Pathological heterogeneity of frontotemporal lobar degeneration with ubiquitin-positive inclusions delineated by ubiquitin immunohistochemistry and novel monoclonal antibodies. *Am J Pathol* 2006;169:1343–52.
- [25] Mackenzie IR, Baborie A, Pickering-Brown S, Du Plessis D, Jaros E, Perry RH, et al. Heterogeneity of ubiquitin pathology in frontotemporal lobar degeneration: classification and relation to clinical phenotype. *Acta Neuropathol* 2006;112:539–49.
- [26] Cairns NJ, Bigio EH, Mackenzie IR, Neumann M, Lee VM, Hatanpaa KJ, et al. Neuropathologic diagnostic and nosologic criteria for frontotemporal lobar degeneration: consensus of the Consortium for Frontotemporal Lobar Degeneration. *Acta Neuropathol* 2007;114:5–22.
- [27] Mackenzie IR, Neumann M, Bigio EH, Cairns NJ, Alafuzoff I, Kriil J, et al. Nomenclature for neuropathologic subtypes of frontotemporal lobar degeneration: consensus recommendations. *Acta Neuropathol* 2009;117:15–8.
- [28] Nakashima-Yasuda H, Uryu K, Robinson J, Xie SX, Hurtig H, Duda JE, et al. Comorbidity of TDP-43 proteinopathy in Lewy body related diseases. *Acta Neuropathol* 2007;114:221–9.
- [29] Uryu K, Nakashima-Yasuda H, Forman MS, Kwong LK, Clark CM, Grossman M, et al. Concomitant TAR-DNA-binding protein 43 pathology is present in Alzheimer disease and corticobasal degeneration but not in other tauopathies. *J Neuropathol Exp Neurol* 2008;67:555–64.
- [30] Davidson Y, Amin H, Kelley T, Shi J, Tian J, Kumaran R, et al. TDP-43 in ubiquitinated inclusions in the inferior olives in frontotemporal lobar degeneration and in other neurodegenerative diseases: a degenerative process distinct from normal ageing. *Acta Neuropathol* 2009;118:359–69.
- [31] Josephs KA, Stroh A, Dugger B, Dickson DW. Evaluation of subcortical pathology and clinical correlations in FTLD-U subtypes. *Acta Neuropathol* 2009;118:349–58.
- [32] Piao YS, Hayashi S, Hasegawa M, Wakabayashi K, Yamada M, Yoshimoto M, et al. Co-localization of alpha-synuclein and phosphorylated tau in neuronal and glial cytoplasmic inclusions in a patient with multiple system atrophy of long duration. *Acta Neuropathol* 2001;101:285–93.
- [33] Ferrer I, Gomez-Isla T, Puig B, Freixes M, Ribe E, Dalfo E, et al. Current advances on different kinases involved in tau phosphorylation, and implications in Alzheimer's disease and tauopathies. *Curr Alzheimer Res* 2005;2:3–18.
- [34] Luna-Munoz J, Chavez-Macias L, Garcia-Sierra F, Mena R. Earliest stages of tau conformational changes are related to the appearance of a sequence of specific phospho-dependent tau epitopes in Alzheimer's disease. *J Alzheimers Dis* 2007;12:365–75.
- [35] Obi K, Akiyama H, Kondo H, Shimomura Y, Hasegawa M, Iwatsubo T, et al. Relationship of phosphorylated alpha-synuclein and tau accumulation to Abeta deposition in the cerebral cortex of dementia with Lewy bodies. *Exp Neurol* 2008;210:409–20.
- [36] Cook C, Zhang YJ, Xu YF, Dickson DW, Petrucelli L. TDP-43 in neurodegenerative disorders. *Expert Opin Biol Ther* 2008;8:969–78.
- [37] Schwab C, Arai T, Hasegawa M, Yu S, McGeer PL. Colocalization of transactivation-responsive DNA-binding protein 43 and huntingtin in inclusions of Huntington disease. *J Neuropathol Exp Neurol* 2008;67:1159–65.
- [38] Saito Y, Kawashima A, Ruberu NN, Fujiwara H, Koyama S, Sawabe M, et al. Accumulation of phosphorylated alpha-synuclein in aging human brain. *J Neuropathol Exp Neurol* 2003;62:644–54.
- [39] Tanabe Y, Ishizu H, Ishiguro K, Itoh N, Terada S, Haraguchi T, et al. Tau pathology in diffuse neurofibrillary tangles with calcification (DNFC): biochemical and immunohistochemical investigation. *NeuroReport* 2000;11:2473–7.
- [40] Josephs KA, Whitwell JL, Knopman DS, Hu WT, Stroh DA, Baker M, et al. Abnormal TDP-43 immunoreactivity in AD modifies clinicopathologic and radiologic phenotype. *Neurology* 2008;70:1850–7.
- [41] Yokota O, Tsuchiya K, Arai T, Yagishita S, Matsubara O, Mochizuki A, et al. Clinicopathological characterization of Pick's disease versus frontotemporal lobar degeneration with ubiquitin/TDP-43-positive inclusions. *Acta Neuropathol* 2009;117:429–44.
- [42] Grossman M. Primary progressive aphasia: clinicopathological correlations. *Nat Rev Neurol* 2010; 6:88–97.
- [43] Deramecourt V, Lebert F, Debachy B, Mackowiak-Cordoliani MA, Bombois S, Kerdraon O, et al. Prediction of pathology in primary progressive language and speech disorders. *Neurology* 2010; 74:42–49.
- [44] Velakoulis D, Walterfang M, Mocellin R, Pantelis C, Dean B, McLean C. Abnormal hippocampal distribution of TDP-43 in patients with-late onset psychosis. *Aust N Z J Psychiatry* 2009;43:739–45.
- [45] Nomoto N, Sugimoto H, Iguchi H, Kurihara T, Wakata N. A case of Fahr's disease presenting "diffuse neurofibrillary tangles with calcification". *Rinsho Shinkeigaku* 2002;42:745–9.
- [46] Langlois NE, Grieve JH, Best PV. Changes of diffuse neurofibrillary tangles with calcification (DNFC) in a woman without evidence of dementia. *J Neurol Neurosurg Psychiatry* 1995;59:103.
- [47] Hempel A, Henze M, Berghoff C, Garcia N, Ody R, Schroder J. PET findings and neuropsychological deficits in a case of Fahr's disease. *Psychiatry Res* 2001;108:133–40.
- [48] Konupckova K, Masopust J, Valis M, Horacek J. Dementia in a patient with Fahr's disease. *Neuro Endocrinol Lett* 2008;29:431–4.
- [49] Ostling S, Andreasson LA, Skoog I. Basal ganglia calcification and psychotic symptoms in the very old. *Int J Geriatr Psychiatry* 2003;18:983–7.



Contents lists available at ScienceDirect

Journal of the Neurological Sciences

journal homepage: www.elsevier.com/locate/jns

FALS with Gly72Ser mutation in SOD1 gene: Report of a family including the first autopsy case

Zen Kobayashi^{a,b,*}, Kuniaki Tsuchiya^a, Takayuki Kubodera^b, Noriyuki Shibata^c,
Tetsuaki Arai^{a,d}, Hiroyuki Miura^e, Chieko Ishikawa^f, Hiromi Kondo^a, Hideki Ishizu^g,
Haruhiko Akiyama^a, Hidehiro Mizusawa^b

^a Department of Psychogeriatrics, Tokyo Institute of Psychiatry, 2-1-8 Kamikitazawa, Setagaya-ku, Tokyo, 156-8585, Japan

^b Department of Neurology and Neurological Science, Graduate School, Tokyo Medical and Dental University, Tokyo, 113-8519, Japan

^c Department of Pathology, Tokyo Women's Medical University, Tokyo, 162-8666, Japan

^d Department of Psychiatry, Graduate School of Comprehensive Human Sciences, University of Tsukuba, Ibaraki, 305-8575, Japan

^e Department of Internal medicine, Ichihara Hospital, Ibaraki, 300-3295, Japan

^f Department of Neurology, Chiba-East National Hospital, Chiba, 260-8712, Japan

^g Department of Laboratory Medicine, Zikei Institute of Psychiatry, Okayama, 702-8508, Japan

ARTICLE INFO

Article history:

Received 31 August 2010

Received in revised form 23 October 2010

Accepted 28 October 2010

Available online 16 November 2010

Keywords:

Familial amyotrophic lateral sclerosis (FALS)

Cu/Zn superoxide dismutase-1 (SOD1)

Gly72Ser

Onuf's nucleus

Hyaline inclusion

ABSTRACT

Clinical information on familial amyotrophic lateral sclerosis (FALS) with Gly72Ser mutation in the Cu/Zn superoxide dismutase-1 (SOD1) gene has been limited and autopsy findings remain to be clarified. We describe one Japanese family with ALS carrying Gly72Ser mutation in the SOD1 gene, in which autopsy was performed on one affected member. The autopsied female patient developed muscle weakness of the left thigh at age 66 and showed transient upper motor neuron signs. She died of respiratory failure 13 months after onset without artificial respiratory support. There were no symptoms suggesting bladder or rectal dysfunction throughout the clinical course. Her brother with ALS was shown to have Gly72Ser mutation in the SOD1 gene. Histopathologically, motor neurons were markedly decreased throughout the whole spinal cord, whereas corticospinal tract involvement was very mild and was demonstrated only by CD68 immunohistochemistry. Degeneration was evident in the posterior funiculus, Clarke's nucleus, posterior cerebellar tract, and Onuf's nucleus. Neuronal hyaline inclusions were rarely observed in the neurons of the spinal cord anterior horn including Onuf's nucleus, and were immunoreactive for SOD1. To date, neuron loss in Onuf's nucleus has hardly been seen in ALS, except in the patients showing prolonged disease duration with artificial respiratory support. Involvement of Onuf's nucleus may be a characteristic pathological feature in FALS with Gly72Ser mutation in the SOD1 gene.

© 2010 Elsevier B.V. All rights reserved.

1. Introduction

Amyotrophic lateral sclerosis (ALS) is a fatal neurodegenerative disorder that mainly involves the upper and lower motor neurons. Familial cases account for 5–10% of all cases of ALS, and mutations of the Cu/Zn superoxide dismutase-1 (SOD1) gene, which encodes an antioxidant enzyme, are present in about 20% of FALS patients and in about 2% of sporadic ALS (SALS) patients [1]. Over 150 mutations in the SOD1 gene have been identified in FALS and SALS cases since 1993 [2]. Within the cell, SOD1 is physiologically distributed in the cytosol, lysosomes, microsomes, mitochondria, and nuclei [3]. Misfolding and aggregation of SOD1 is related to gain of toxic function in ALS with SOD1 mutation [4]. Increasing evidence indicates that non-neuronal-

neighboring cell types contribute to the pathogenesis and disease progression [5].

Clinical features of ALS with SOD1 mutation are largely indistinguishable from those of SALS; however, lower limb-onset and lower motor neuron-predominant involvement are relatively common [6]. The onset age and disease duration are variable among the mutations. Histopathologically, most cases of ALS with SOD1 mutation show Lewy body-like hyaline inclusions, which are immunoreactive for SOD1 [7–9]. The posterior funiculus, Clarke's nucleus and posterior spinocerebellar tract were also involved. The corticospinal tract (CST) involvement is slight or mild [7]. In patients with the I113T mutation, neurofilament pathology is an almost universal feature [7].

Onuf's nucleus is a small group of cells, first described by a neuroanatomist called Onufrowicz. In 1899, he found that this group of cells was localized exclusively in the second sacral segment [10]. Onuf's nucleus is functionally related to the rectum and bladder, including the external sphincter muscles of the anus and urethra [10].

* Corresponding author. Department of Psychogeriatrics, Tokyo Institute of Psychiatry, 2-1-8 Kamikitazawa, Setagaya-ku, Tokyo, 156-8585, Japan.

E-mail address: zen@bg7.so-net.ne.jp (Z. Kobayashi).

Onuf's nucleus is usually preserved in ALS [10,11], and neuron loss has hardly been seen except in the patients showing prolonged disease duration with artificial respiratory support [12–15]. Here, we report one Japanese family with ALS showing Gly72Ser mutation including the first autopsy patient, in whom both neuron loss and neuronal cytoplasmic inclusions were demonstrated in Onuf's nucleus.

2. Clinical assessment

2.1. Case II-2

The family tree is shown in Fig. 1. A 75-year-old Japanese man developed muscle weakness of the fingers of the bilateral upper limbs. There had been paresis of the right upper limb since brain infarction occurred at age 65. Two patients with ALS in his family had already died (Fig. 1). Six months after onset, muscle weakness emerged at the proximal parts of the bilateral upper limbs, and nine months after onset, he became unable to produce vocal sounds. He was admitted to the Department of Neurology in the general hospital ten months after onset. On admission, there was marked tongue atrophy and fasciculation, and prominent dysarthria. Neck weakness corresponded to grade 3 in the manual muscle testing. Symmetrical muscle weakness of the bilateral upper limbs ranged from grades 3 to 4 on manual muscle testing. There was no muscle weakness in the lower limbs. Deep tendon reflex was increased in the right upper limb and bilateral lower limbs. Plantar reflexes were not elicited. There was no sensory disturbance. Needle electromyography detected active and chronic denervation potentials, and a diagnosis of familial ALS was made. DNA was extracted from his blood sample, and direct sequencing of SOD1 gene exon 3 showed missense mutation substituting glycine for serine (Gly72Ser) (Fig. 2). He died of respiratory failure ten months after onset. Autopsy could not be performed.

2.2. Case II-4

A 66-year-old woman developed muscle weakness of the left thigh, and experienced falls. Two months after onset, fasciculation emerged in the muscles of the left thigh. Four months after onset, she needed a cane while walking, then became unable to walk and was admitted to a general hospital five months after onset. On admission, there were muscle fasciculations in the bilateral thigh and hip, and muscle atrophy and weakness in the left lower limb. Muscle weakness ranged from grades 0 to 2 on manual muscle testing. Achilles tendon reflex was absent on the left side, and was within normal limits on the right. The patellar tendon reflex was decreased on the left side and increased on the right. The upper limbs tendon reflex was bilaterally increased. There was Babinski's sign bilaterally. Vibration sensation was slightly decreased in the bilateral lower limbs. On nerve

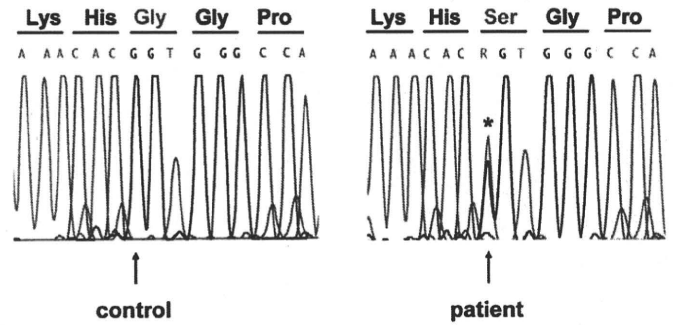


Fig. 2. Direct sequencing of SOD1 gene exon 3 showed missense mutation substituting glycine for serine (Gly72Ser).

conduction study, there was no conduction block. Needle electromyography showed denervation potentials in the bilateral lower limbs and right upper limb. A diagnosis of ALS was made. At that time, information on the family history of ALS could not be obtained. Thereafter, muscle weakness emerged in the right lower limb.

Seven months after onset, neurological examination demonstrated flaccid paraparesis without hyperreflexia or plantar reflexes. Nerve conduction study demonstrated reduction of the amplitude of the compound muscle action potentials (CMAPs), but conduction velocity was within normal limits. Cerebrospinal fluid examination showed slight elevation of the total protein level (53 mg/dl). Because we could not completely exclude the possibility of chronic inflammatory demyelinating polyradiculoneuropathy (CIDP), prednisolone of 60 mg was administered for six months. However, there was no improvement.

About ten months after onset, muscle weakness emerged in the trunk and upper limbs, and non-invasive positive pressure ventilation was initiated. At that time, neurological examination demonstrated lower-limb dominant tetraparesis and absence of the tendon reflex in the bilateral lower limbs. There was no facial palsy, dysarthria, dysphasia, or tongue atrophy. Nerve conduction study demonstrated marked reduction of the amplitude of the CMAPs in the four limbs (<0.3 mV), but conduction velocity remained within normal limits. Muscle action potentials were not detected in the right tibial nerve or left ulnar nerve. Sensory nerve action potentials (SNAPs) were within normal limits. The patient refused artificial respiratory support and died of respiratory failure 13 months after onset. There were no symptoms suggesting bladder or rectal dysfunction throughout the clinical course. Genetic sequencing could not be performed.

2.3. Case II-6

This patient was also diagnosed as having ALS and died at age 39, but information other than this could not be obtained.

Table 1 Antibodies used for immunohistochemistry.

Antibody	Type	Source	Dilution
Anti-ubiquitin	Rabbit polyclonal	Dako, Glostrup, Denmark	1:2000
Anti-p62 (SQSTM1)	Rabbit polyclonal	Biomol, Philadelphia, PA, USA	1:1000
Anti-TDP-43	Rabbit polyclonal	Proteintech Group, Chicago, IL, USA	1:1000
Anti-SOD1	Rabbit polyclonal	Made by Asayama et al. [21]	1:20,000
Anti-neurofilament (SMI 31)	Mouse monoclonal	Sternberger, Lutherville, MD, USA	1:1000
Anti-CD68	Mouse monoclonal	Dako, Glostrup, Denmark	1:100

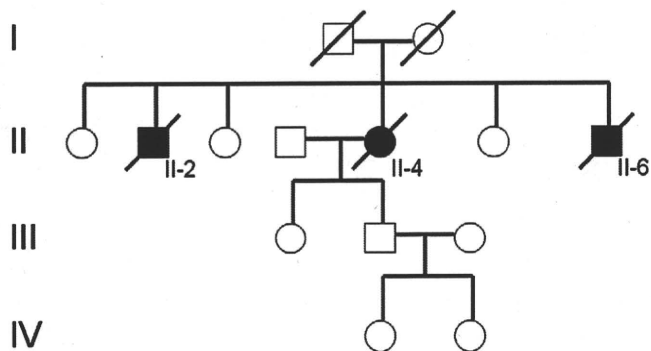


Fig. 1. Pedigree of a Japanese family with FALS harboring Gly72Ser mutation in the SOD1 gene. Males are represented by square, females by circles. Affected members are represented by solid symbols, deceased individuals by diagonals.

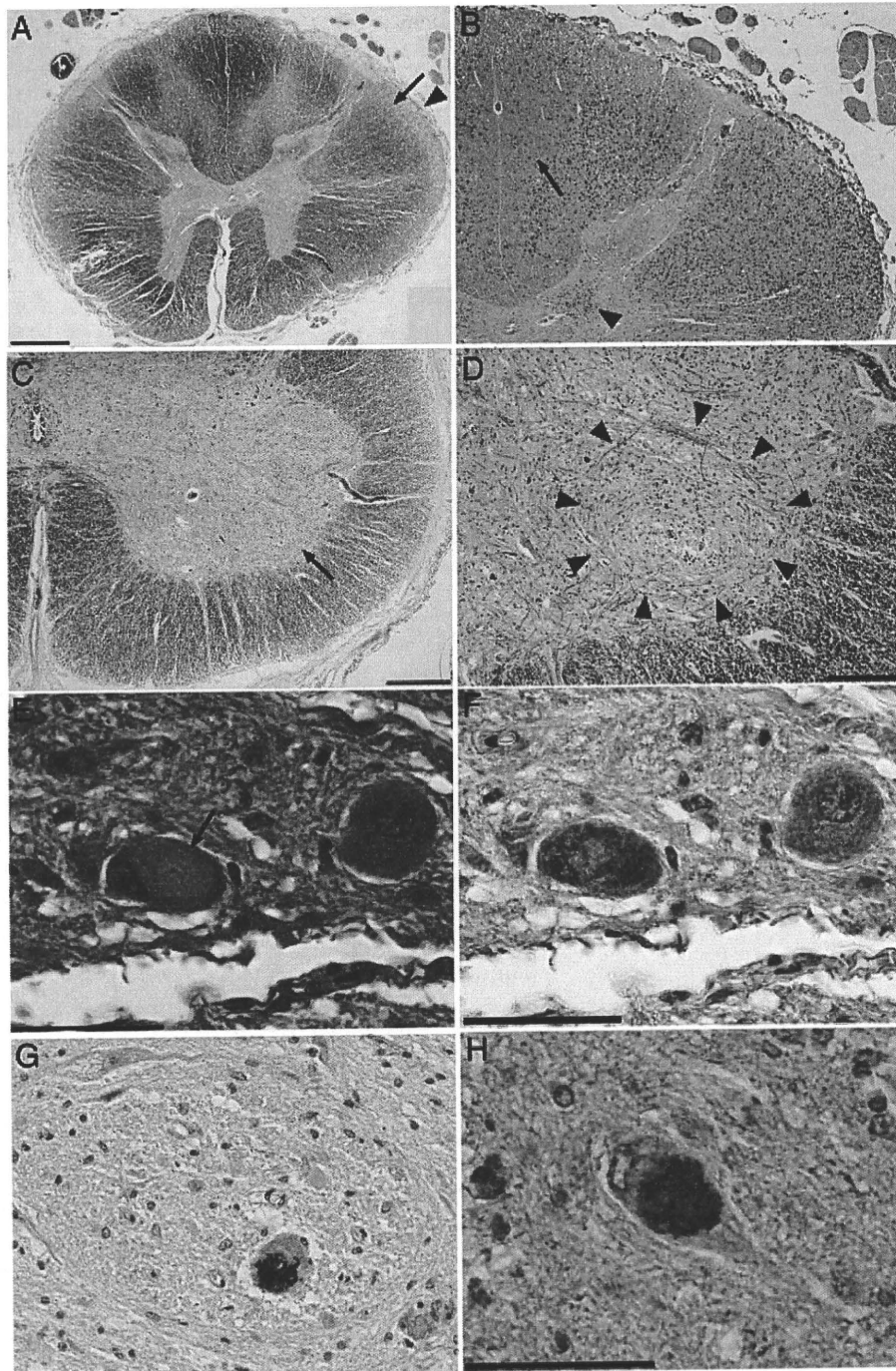


Fig. 3. (A) and (B) are serial sections. A. In the lower thoracic cord, the central portion of the posterior funiculus was involved with left predominance, and the posterior intermediate sulci could not be identified. Although the subpial region was not well stained by KB staining, myelin pallor was evident in the posterior cerebellar tract (arrowhead). The corticospinal tract (CST) involvement was not apparent (arrow). B. CD68 immunohistochemistry of the left lateral and posterior funiculi showed proliferation of activated macrophages/microglia in the CST, Clarke's nucleus (arrowhead), posterior cerebellar tract and posterior funiculus. In the posterior funiculus, the region around the posterior central sulcus (arrow) was almost intact. C. Marked neuronal loss was observed in the anterior horn of the left second sacral segment. The arrow indicates Onuf's nucleus. D. A high-power view of the left Onuf's nucleus (arrowheads) demonstrated severe neuron loss. E, F. The hyaline inclusion (E, arrow) in a neuron of Onuf's nucleus demonstrated by HE staining was partially immunoreactive for SOD1 (F). The nucleus was located in the periphery. G. The left Onuf's nucleus is shown. Using p62 immunohistochemistry, the inclusion in the remaining neuron of Onuf's nucleus were labeled. H. The other inclusion immunoreactive for SOD1 in the remaining neuron of the anterior horn of the second sacral segment. Scale bars = 1 mm (A), 500 μ m (C), 200 μ m (D), and 50 μ m (E–H).

3. Methods

Brain and spinal cord tissue samples of case II-4 were fixed postmortem with 10% formalin and embedded in paraffin. Ten-micrometer-thick (Multiple 10- μ m-thick) sections were prepared from the cerebrum, midbrain, pons, medulla oblongata, cerebellum, and spinal cord including the cervical, thoracic, lumbar and sacral

segments. These sections were stained with hematoxylin–eosin (HE) and Klüver–Barrera (KB) and by the Bodian impregnation method. Spinal cord sections were examined immunohistochemically by the immunoperoxidase method using 3,3'-diaminobenzidine tetrahydrochloride and hematoxylin as the chromogen and counterstain, respectively. Antibodies used in this study are shown in Table 1.

Table 2
Clinical features of familial amyotrophic lateral sclerosis with Gly72Ser mutation in the SOD1 gene.

	Age at onset/Gender	Age at death	Site of onset	Atypical features	Disease penetrance in the family
Orrell et al. III-3 [16]	47/M	51	Right foot	Decreased vibration sensation, No UMN signs	Incomplete
Orrell et al. III-8 [16]	46 or 47/F	49	Legs	ND	
Shaw et al. [17]	29/M	30 or 31	Left thigh	No family history	Incomplete
Present case II-2	75/M	76	Upper limbs	ND	Incomplete
Present case II-4	66/F	67	Left thigh	Decreased vibration sensation, Limited UMN signs	
Present case II-6	ND/M	39	ND	ND	

M male, F female, UMN upper motor neuron, ND not described.

4. Results

4.1. Neuropathological findings

Brain weight was 1225 g after fixation. Macroscopically, there were no abnormalities in the brain. The anterior roots of the spinal cord were atrophic. Microscopically, as previously reported in ALS cases showing SOD1 mutation, the posterior funiculus was involved throughout the whole spinal cord, and the posterior cerebellar tract was also affected in the thoracic and cervical cord (Fig. 3A, B). In the thoracic cord, neurons of Clarke's nucleus were depleted, whereas the intermediolateral nucleus was preserved. The CST involvement was not apparent by KB staining (Fig. 3A). Severe neuron loss was observed in the anterior horn of the whole spinal cord (Fig. 3C). The number of neurons in Onuf's nucleus were slightly decreased on the right side, and markedly decreased on the left (Fig. 3D). This finding was confirmed on ten serial sections. Neuronal hyaline inclusions were rarely observed in the remaining neurons of the spinal cord anterior horn including Onuf's nucleus (Fig. 3E). There were no apparent astrocytic hyaline inclusions [13]. In the brainstem, neuronal loss was slight in the hypoglossal nucleus, and was not apparent in the motor nucleus of the trigeminal nerve. There were no Bunina bodies. There was no apparent neuronal loss in the cerebrum or cerebellum including the primary motor cortex, although the neurons in these regions frequently showed ischemic changes related to hypoxia in the terminal stage of the disease.

4.2. Immunohistochemical findings

Although the CST involvement was not apparent by myelin stain as described above, CD68 immunohistochemistry demonstrated proliferation of activated macrophages/microglia in the CST (Fig. 3B). CD68 immunohistochemistry also showed involvement of the posterior cerebellar tract, Clarke's nucleus (Fig. 3B), and inferior cerebellar peduncle of the medulla oblongata. Ubiquitin, p62, and SOD1 immunohistochemistry demonstrated neuronal cytoplasmic inclusions in the remaining neurons of the spinal cord anterior horn including Onuf's nucleus (Fig. 3F–H). Immunoreactivity for neurofilament or TDP-43 was not apparent in the inclusions. Onuf's nucleus sections containing hyaline inclusions were first stained with HE, and photographed, and then destained in ethanol, and finally immunostained for SOD1. Hyaline inclusions in the remaining neurons of Onuf's nucleus identified by HE staining (Fig. 3E) were partially and irregularly immunoreactive for SOD1 (Fig. 3F).

5. Discussion

The clinical features of FALS with Gly72 Ser mutation in the SOD1 gene is summarized in Table 2. Unlike previous reports [16,17], our cases II-2 and II-4 showed disease onset in the sixth or seventh decade. In addition, case II-2 developed weakness of the upper limbs, and the lower limbs were well preserved throughout the clinical course. These findings indicate that the same Gly72Ser mutation may

present different clinical courses, even within the same family. In case II-4 (autopsied patient), neurological examination had shown decreased vibration sensation in the lower limbs although the patient did not complain of sensory symptoms. Additionally, we could not clinically exclude the possibility of CIDP in this patient because the upper motor neuron signs were limited. In the view of clinicopathological correlation, impaired vibration sensation may be due to posterior funiculus involvement, and limited upper motor neuron signs appeared to reflect mild CST involvement.

Neuropathologically, many SOD1-mutated FALS cases show neuronal Lewy body-like hyaline inclusions. In addition, long surviving FALS patients with SOD1 gene mutations present with astrocytic hyaline inclusions [7]. These neuronal and astrocytic inclusions contain both wild-type and mutant SOD1 protein. In some mutations, however, SOD1 aggregation is not demonstrated histopathologically [7], therefore the process of neuron death may somewhat differ among the mutations. Further study is required to clarify the process of neuronal degeneration in ALS with SOD1 mutation.

The salient pathological feature in case II-4 was neuron loss in Onuf's nucleus, although clinical symptoms suggesting bladder or rectal dysfunction were absent. SOD1 aggregation demonstrated in the remaining neurons of Onuf's nucleus suggests that Onuf's nucleus was involved in the disease process associated with Gly72Ser mutation. To date, Onuf's nucleus has been considered largely intact in ALS [10,11], and neuron loss has hardly been seen except in patients showing prolonged disease duration with artificial respiratory support [12–15]. Exceptionally, Yoshida et al [18] and Kihira et al [19] reported a FALS case and a SALS case respectively, showing neuron loss in Onuf's nucleus despite disease duration shorter than three years. In the other study, Kihira et al. showed Bunina bodies and ubiquitin-immunoreactive inclusions in the neurons of Onuf's nucleus in some ALS cases while neuron loss was not apparent [20]. They concluded that Onuf's nucleus is involved in the disease process in some ALS cases, although the severity of degeneration was of a lesser degree than that in other motor nuclei. Among ALS cases showing the SOD1 mutation, neuron loss with neuronal and glial inclusions in Onuf's nucleus was reported only in one patient with two base pair deletion in codon 126 of exon 5 [13], who showed a prolonged disease duration with artificial respiratory support.

In conclusion, the findings in this family provide new information regarding the clinicopathological features of FALS with Gly72Ser mutation in the SOD1 gene. Further clinicopathological information in a larger number of cases showing Gly72Ser mutation is needed to clarify whether involvement of Onuf's nucleus is associated with this mutation.

Acknowledgements

This work was supported by Grants-in-Aid from the Ministry of Health, Labour and Welfare of Japan, Grants-in-Aid for scientific research from the Ministry of Education, Culture, Sports, Science and Technology (14570957) and a research grant from the Zikei Institute of Psychiatry.

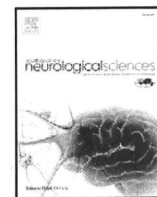
References

- [1] Wijesekera LC, Leigh PN. Amyotrophic lateral sclerosis. *Orphanet J Rare Dis* 2009;4:3.
- [2] Battistini S, Ricci C, Lotti EM, Benigni M, Gagliardi S, Zucco R, et al. Severe familial ALS with a novel exon 4 mutation (L106F) in the SOD1 gene. *J Neurol Sci* 2010;293:112–5.
- [3] Okado-Matsumoto A, Fridovich I. Subcellular distribution of superoxide dismutases (SOD) in rat liver: Cu,Zn-SOD in mitochondria. *J Biol Chem* 2001;276:38388–93.
- [4] Kerman A, Liu HN, Croul S, Bilbao J, Rogaeva E, Zinman L, et al. Amyotrophic lateral sclerosis is a non-amyloid disease in which extensive misfolding of SOD1 is unique to the familial form. *Acta Neuropathol* 2010;119:335–44.
- [5] Ilieva H, Polymenidou M, Cleveland DW. Non-cell autonomous toxicity in neurodegenerative disorders: ALS and beyond. *J Cell Biol* 2009;187:761–72.
- [6] Aoki M, Warita H, Itoyama Y. Amyotrophic lateral sclerosis with the SOD1 mutations. *Rinsho Shinkeigaku* 2008;48:966–9.
- [7] Kato S. Amyotrophic lateral sclerosis models and human neuropathology: similarities and differences. *Acta Neuropathol* 2008;115:97–114.
- [8] Shibata N, Hirano A, Kobayashi M, Siddique T, Deng HX, Hung WY, et al. Intense superoxide dismutase-1 immunoreactivity in intracytoplasmic hyaline inclusions of familial amyotrophic lateral sclerosis with posterior column involvement. *J Neuropathol Exp Neurol* 1996;55:481–90.
- [9] Shibata N, Hirano A, Yamamoto T, Kato Y, Kobayashi M. Superoxide dismutase-1 mutation-related neurotoxicity in familial amyotrophic lateral sclerosis. *Amyotroph Lateral Scler Other Mot Neuron Disord* 2000;1:143–61.
- [10] Mannen T. Neuropathological findings of Onuf's nucleus and its significance. *Neuropathology* 2000;20:S30–3.
- [11] Mannen T, Iwata M, Toyokura Y, Nagashima K. Preservation of a certain motoneuron group of the sacral cord in amyotrophic lateral sclerosis: its clinical significance. *J Neurol Neurosurg Psychiatry* 1977;40:464–9.
- [12] Kato S, Hayashi H, Oda M, Kawata A, Shimizu T, Hayashi M, et al. Neuropathology in sporadic ALS patients on respirators. In: Nakano I, Hirano A, editors. *Amyotrophic Lateral Sclerosis: Progress and Perspectives in Basic Research and Clinical Application*. Amsterdam: Elsevier; 1996. p. 66–77.
- [13] Kato S, Shimoda M, Watanabe Y, Nakashima K, Takahashi K, Ohama E. Familial amyotrophic lateral sclerosis with a two base pair deletion in superoxide dismutase 1: gene multisystem degeneration with intracytoplasmic hyaline inclusions in astrocytes. *J Neuropathol Exp Neurol* 1996;55:1089–101.
- [14] Shimizu T, Kawata A, Kato S, Hayashi M, Takamoto K, Hayashi H, et al. Autonomic failure in ALS with a novel SOD1 gene mutation. *Neurology* 2000;54:1534–7.
- [15] Tateishi T, Hokenohara T, Yamasaki R, Miura S, Kikuchi H, Iwaki A, et al. Multiple system degeneration with basophilic inclusions in Japanese ALS patients with FUS mutation. *Acta Neuropathol* 2010;119:355–64.
- [16] Orrell RW, Marklund SL, deBelleruche JS. Familial ALS is associated with mutations in all exons of SOD1: a novel mutation in exon 3 (Gly72Ser). *J Neurol Sci* 1997;153:46–9.
- [17] Shaw CE, Enayat ZE, Chioza BA, Al-Chalabi A, Radunovic A, Powell JF, et al. Mutations in all five exons of SOD-1 may cause ALS. *Ann Neurol* 1998;43:390–4.
- [18] Yoshida M, Okuda S, Murakami N, Hashizume Y, Sobue G. Two siblings of familial amyotrophic lateral sclerosis with multisystemic degeneration characterized by mild involvement of the middle root zone of the posterior column, Clarke's nuclei and spinocerebellar tract. *Rinsho Shinkeigaku* 1995;35:589–99.
- [19] Kihira T, Mizusawa H, Tada J, Namikawa T, Yoshida S, Yase Y. Lewy body-like inclusions in Onuf's nucleus from two cases of sporadic amyotrophic lateral sclerosis. *J Neurol Sci* 1993;115:51–7.
- [20] Kihira T, Yoshida S, Yoshimasu F, Wakayama I, Yase Y. Involvement of Onuf's nucleus in amyotrophic lateral sclerosis. *J Neurol Sci* 1997;147:81–8.
- [21] Asayama K, Janco RL, Burr IM. Selective induction of manganese superoxide dismutase in human monocytes. *Am J Physiol* 1985;249:C393–7.



Contents lists available at ScienceDirect

Journal of the Neurological Sciences

journal homepage: www.elsevier.com/locate/jns

Clinicopathological characteristics of FTLD-TDP showing corticospinal tract degeneration but lacking lower motor neuron loss

Zen Kobayashi ^{a,b,*}, Kuniaki Tsuchiya ^a, Tetsuaki Arai ^{a,c}, Osamu Yokota ^d, Mari Yoshida ^e, Yoko Shimomura ^a, Hiromi Kondo ^a, Chie Haga ^a, Toshiyasu Asaoka ^f, Mitsumoto Onaya ^f, Hideki Ishizu ^g, Haruhiko Akiyama ^a, Hidehiro Mizusawa ^b

^a Department of Psychogeriatrics, Tokyo Institute of Psychiatry, 2-1-8 Kamikitazawa, Setagaya-ku, Tokyo 156-8585, Japan

^b Department of Neurology and Neurological Science, Graduate School, Tokyo Medical and Dental University, Tokyo 113-8519, Japan

^c Department of Psychiatry, Graduate School of Comprehensive Human Sciences, University of Tsukuba, Ibaraki 305-8577, Japan

^d Department of Neuropsychiatry, Okayama University Graduate School of Medicine, Dentistry and Pharmaceutical Sciences, Okayama 700-8558, Japan

^e Department of Neuropathology, Institute for Medical Science of Aging, Aichi Medical University, Aichi 480-1195, Japan

^f National Hospital Organization Shimofusa Psychiatric Medical Center, Chiba 266-0007, Japan

^g Department of Laboratory Medicine, Zikei Institute of Psychiatry, Okayama 702-8508, Japan

ARTICLE INFO

Article history:

Received 1 June 2010

Received in revised form 30 July 2010

Accepted 6 August 2010

Keywords:

FTLD-TDP

Motor neuron disease

Amyotrophic lateral sclerosis

Primary lateral sclerosis

Corticospinal tract

ABSTRACT

The presence of frontotemporal lobar degeneration with TDP-43-positive inclusions (FTLD-TDP) showing corticospinal tract (CST) degeneration but lacking lower motor neuron (LMN) loss has been reported, and the term primary lateral sclerosis (PLS) is used to distinguish motor neuron disease (MND) of these cases from amyotrophic lateral sclerosis (ALS). To date, however, details of clinicopathological findings of FTLD-MND-PLS type (FTLD-MND-P) have not been reported. We evaluated medical records and histopathological findings of ten cases of FTLD-MND-P, in comparison with those of six FTLD-MND-ALS type (FTLD-MND-A) cases. The mean age at onset and disease duration of FTLD-MND-P cases were 54 and 12 years, respectively. The first symptoms were frontotemporal dementia showing behavioral abnormality and/or personality change in five cases, semantic dementia in three cases, progressive non-fluent aphasia in one case, and auditory hallucination in one case. Upper motor neuron signs were clinically identified in six of the ten cases. There were no LMN signs throughout the clinical course in any case. Histopathologically, there was no obvious LMN loss or Bunina bodies in the hypoglossal nucleus or spinal cord in any case, whereas the CST was involved in all cases. The cerebral cortex of the six cases showed type 1 of TDP-43 histology defined by Cairns et al., whereas three cases showed type 3 histology, and one case showed type 2 histology. In all cases, TDP-43 positive neuronal cytoplasmic inclusions were absent or rare in the LMNs, while TDP-43 positive round structures were frequently identified in the neuropil of the spinal cord anterior horn in some cases. This study clarified that FTLD-MND-P cases have characteristic clinicopathological features distinct from those of FTLD-MND-A.

© 2010 Elsevier B.V. All rights reserved.

1. Introduction

Clinical phenotypes of FTLD-TDP include frontotemporal dementia (FTD) showing behavioral abnormality and/or personality change, semantic dementia (SD), and progressive non-fluent aphasia (PA). The most common subtype of FTLD-TDP is FTD [1,2], and a proportion of patients with FTD develops motor neuron disease (MND), which usually refers to amyotrophic lateral sclerosis (ALS) [3].

Definitions of FTLD with MND (FTLD-MND) and ALS with dementia (ALSD) are dependent on which symptoms present first [4]. The disease duration of FTLD-MND is about 44 months, whereas that of ALSD is about 34 months [5]. Exceptionally, an FTLD-MND case showing a disease duration of 11 years and TDP-43-positive neuronal cytoplasmic inclusions (NCIs) in the cerebral cortex was reported [6,7]. In FTLD-MND, personality changes are usually mild [8], and SD or PA is hardly seen. The bulbar regions and upper limbs are preferentially affected, and the hypoglossal nucleus usually shows neuronal loss [8].

There are four subtypes of TDP-43 histology in the cerebral cortex of FTLD-TDP [9]. Type 1 histology is characterized by an abundance of dystrophic neurites (DNs) predominantly in the superficial cortical

* Corresponding author. Department of Psychogeriatrics, Tokyo Institute of Psychiatry, 2-1-8 Kamikitazawa, Setagaya-ku, Tokyo, 156-8585, Japan. Tel.: +81 3 3304 5701; fax: +81 3 3329 8035.

E-mail address: zen@bg7.so-net.ne.jp (Z. Kobayashi).

layers, with few NCIs. Glial cytoplasmic inclusions (GCIs) are rare. Type 2 histology shows abundant NCIs in both the superficial and deep cortical layers with few DNs. GCIs are frequently seen in the gray and white matter. Type 3 histology presents with mixed or intermediate histology of types 1 and 2, namely abundant DNs and NCIs predominantly in the superficial cortical layers. Neuronal intranuclear inclusions (NIIs) are occasionally seen, and GCIs are often present. These histological subtypes correspond to the distinct patterns of immunoblot bands of cleaved TDP-43 [10]. Josephs et al. reported that mutations of the progranulin gene were seen in 35% of cases showing type 3 histology [1] (type 1 histology defined by Mackenzie et al. [11]). FTLD-MND cases show type 2 or 3 histology [9,12]. In general, type 3 is the most common of the four types [1,9,12,13]. The disease duration increases from type 2 to 3, and to 1 [1,12,14], and the duration of type 1 is reported to range from six [14] to ten [1] years.

The corticospinal tract (CST) is the largest and most important descending fiber system, and the CST fibers arise not only from the PMC, but also from the premotor cortex, supplementary motor area, and parietal areas [15]. Recently, the presence of FTLD-TDP showing CST degeneration but lacking LMN loss was reported [1,16,17], and the term primary lateral sclerosis (PLS) is used to distinguish MND of these cases from ALS [1,16]. Josephs et al. reported that the disease duration in two cases of FTLD-MND-PLS type (FTLD-MND-P) was six years and seven years, respectively [16]. They subsequently showed that there were only two cases of FTLD-MND-P among 39 FTLD-TDP cases, and the cerebral cortex of these cases presented with type 1 histology [1] (type 2 histology defined by Mackenzie et al. [11]). In contrast, Yokota et al. recently reported that FTLD-MND-P is not rare among FTLD-TDP cases in Japan [17]. Because details of the clinicopathological findings of FTLD-MND-P have not been reported to date, we evaluated the clinical and histopathological findings focusing on the motor system in ten FTLD-MND-P cases, and compared them with those of six FTLD-MND-ALS type (FTLD-MND-A) cases.

2. Materials and methods

2.1. Subjects

There were 29 cases of FTLD-TDP including 13 women and 16 men pathologically examined in Tokyo Institute of Psychiatry from 1974 to 2009. Some of these cases were reported previously [17–22]. All patients fulfilled the international clinical and pathological diagnostic criteria [3,23]. The clinical information and TDP-43 histology of these 29 cases are shown in Table 1. There were no cases showing a family history of FTLD or type 4 TDP-43 histology. The numbers of cases showing types 1, 2 and 3 were 10, 14 and 5, respectively. Although the cases showing type 3 were rare in our series, this tendency may be

Table 1
FTLD-TDP cases in our institution.

Type of TDP-43 histology	Mean disease duration, y	Clinical phenotype	Number of cases
Type 1	12.7	SD	7 (3)
		FTD	3 (3)
Type 2	2.7	FTD with ALS	5 (0)
		ALSD	4 (0)
		FTD	2 (0)
		SD	2 (0)
Type 3	6.6	PA	1 (1)
		FTD	3 (2)
		FTD with ALS	1 (0)
		unclassifiable	1 (1)

SD semantic dementia, FTD frontotemporal dementia, ALS amyotrophic lateral sclerosis, ALSd ALS with dementia, PA progressive non-fluent aphasia. Parenthesis shows the number of FTLD-MND-P cases.

partly explained by the low frequency of familial cases of FTLD in Japan [24,25]. The mean disease duration of each type was 12.7 years, 2.7 years and 6.6 years, respectively. There were four cases of ALSD that initially showed LMN signs such as muscle atrophy and weakness, followed by dementia. Conversely, there were six cases of FTD with ALS that initially presented with dementia, followed by LMN signs. These cases of ALSD and FTD with ALS showed LMN loss, formation of Bunina bodies, and type 2 TDP-43 histology while one case of FTD with ALS showed type 3 histology. Among 14 cases showing type 2 histology in our institution, all but one case showed variable degrees of LMN loss.

In this study, we defined “FTLD-MND-P” as FTLD-TDP showing CST degeneration but lacking obvious LMN loss or Bunina bodies in the hypoglossal nucleus or spinal cord. Among the 29 FTLD-TDP cases examined in our institution, we first excluded four cases showing type 1 histology because the available tissue was limited. Subsequently, we identified ten FTLD-MND-P cases (cases 1–10, shown in Table 2). At our institution, there was only one FTLD-TDP case showing preservation of both the CST and LMNs in the brain and spinal cord. This case showed an absence of UMN signs throughout the total clinical course of seven years and presented with type 3 TDP-43 histology in the cerebral cortex. For comparison, we examined six FTLD-MND-A cases (cases 11–16, shown in Table 2).

2.2. Conventional neuropathology

Brain tissue samples from all subjects were fixed postmortem with 10% formalin and embedded in paraffin. Hemispheric sections (10 μ m thick) were prepared from the frontal, temporal, parietal, and occipital lobes. Sections of midbrain, pons, medulla oblongata, cerebellum, and cervical, thoracic, and lumbar cord were also prepared when available. In case 3 only, hemispheric sections of the cerebrum were not available. These sections were stained by the hematoxylin–eosin (HE), Klüver–Barrera (KB), Holzer, methenamine silver, Bodian, and Gallyas–Braak methods. A genetic study could not be done because only formalin-fixed and paraffin-embedded tissues were available.

2.3. Assessment of the cerebral cortex and CST

The severity of neuronal loss and gliosis in the cerebral cortex was assessed on HE-, KB-, Bodian- and Holzer-stained sections. The PMC was identified as the cortex where Betz cells were identified. The CST degeneration in the subcortical white matter of the PMC, posterior limb of the internal capsule, cerebral peduncle, and spinal cord was assessed by the evidence of loss of myelin and axons, glial proliferation, and the presence of macrophages, and indicated as – (absent) or + (present). The CST degeneration at the level of the medulla oblongata was assessed according to the grading system of the previous study [17], and was indicated as –: no degeneration (no myelin pallor), 1+: mild degeneration (slight myelin pallor without atrophy of the pyramid), 2+: moderate degeneration (evident myelin pallor with slight atrophy of the pyramid), and 3+: severe degeneration (evident myelin pallor with severe atrophy of the pyramid).

2.4. Immunohistochemistry

Antibodies used in immunohistochemistry are shown in Table 3. Sections from the frontal, temporal and anterior parietal lobes, brainstem, cerebellum, and cervical, thoracic, and lumbar cord were examined using antibodies to TDP-43. Cystatin C immunoreactivity was examined in the brainstem and spinal cord. Deparaffinized sections were incubated with 1% H₂O₂ in methanol for 30 min to eliminate endogenous peroxidase activity in the tissue. When using anti-TDP-43C [405–414], sections were pretreated by autoclaving for

Table 2
Clinical features of the FTLD-MND-P cases (cases 1–10) and FTLD-MND-A cases (cases 11–16).

Case no./sex	Age of onset, y	Onset age of LMN signs, y	Onset age of UMN signs, y	Age at death, y	Disease duration, y	Clinical course	UMN signs	Clinical diagnosis
1/M	47	–	48	50	2.7	FTD, UMN signs	Hyperreflexia (rt), Hemiparesis (rt)	SD?
2/M	75	–	N	81	5.8	PA	N	SPA
3/F	49	–	N	57	8	FTD	N	AD
4/M	52	–	60	61	10	SD, FTD, UMN signs, Parkinsonism	Hyperreflexia (rt), Spasticity (rt), Babinski's sign (rt)	Pick
5/M	52	–	N	63	11	FTD	N	Pick
6/F	48	–	54	60	12	Auditory hallucination, SD, FTD, UMN signs	Hyperreflexia (rt), Babinski's sign (rt)	Pick
7/F	58	–	72	72	14	SD, FTD, UMN signs	Babinski's sign	Pick
8/M	58	–	66	74	16	FTD, SD, Parkinsonism, UMN signs	Hyperreflexia (lt), Babinski's sign, Paralysis of upper limb (lt)	Pick
9/M	55	–	72	74	19	SD, FTD, Parkinsonism, UMN signs	Hyperreflexia, Ankle clonus	SPA
10/F	49	–	N	70	21	FTD	N	Pick
11/M	60	61	–	61	1.7	Memory impairment, FTD, LMN signs	–	Dementia with MND
12/M	63	63	64	65	1.7	FTD, LMN and UMN signs	Hyperreflexia, Babinski's sign	ALSD
13/M	49	50	50	52	3	FTD, SD, LMN and UMN signs	Hyperreflexia	Dementia with MND
14/F	39	39	41	42	3.2	FTD, LMN and UMN signs	Hyperreflexia	Dementia with MND
15/F	54	57	57	58	4	Memory impairment, FTD, LMN and UMN signs	Hyperreflexia	Dementia with MND
16/F	64	70	70	70	6	FTD, LMN and UMN signs	Hyperreflexia	Dementia with MND

–: absent, N: not recorded, rt: right side (or right side predominant), lt: left side (or left side predominant), LMN lower motor neuron, UMN upper motor neuron, FTD frontotemporal dementia, PA progressive non-fluent aphasia, SD Semantic dementia, AD Alzheimer's disease, Pick Pick's disease, SPA Slowly progressive aphasia, MND motor neuron disease, ALSD amyotrophic lateral sclerosis with dementia. In the column of Clinical course, the symptoms are described in the order that they appeared.

10 min in 10 mM sodium citrate buffer at 120 °C. After washing sections with 0.01 M phosphate buffered saline (PBS, pH 7.4) three times for 10-min each, the specimens were blocked with 10% normal serum. Sections were incubated overnight at 4 °C with one of the primary antibodies in 0.05 M Tris-HCl buffer, pH 7.2. After washing three times for 10-min each in PBS, sections were incubated in biotinylated anti-mouse or anti-rabbit secondary antibody for 1 h, and then in avidin-biotinylated horseradish peroxidase complex (ABC Elite kit, Vector) for 1 h. Peroxidase labeling was visualized with 0.2% 3,3'-diaminobenzidine (DAB) as the chromogen. Sections were counterstained with hematoxylin.

2.5. Confocal microscopy

Double labeling immunofluorescence for TDP-43C [405–414] and ubiquitin (mouse, monoclonal, clone MAB1510; 1:200, Millipore, Temecula, CA, USA), and for TDP-43C [405–414] and p62-N (guinea pig, polyclonal; 1:500, PROGEN Biotechnik GmbH, Heidelberg, Germany) was performed on the spinal cord specimen from case 10. After washing with Tx-PBS for 30 min, sections were incubated for 2 h at room temperature in a cocktail of fluorescein isothiocyanate (FITC)-conjugated goat anti-mouse IgG (1:100, Millipore, Temecula, CA) and tetramethylrhodamine isothiocyanate (TRITC)-conjugated goat anti-rabbit IgG (1:100, Millipore). After washing, sections were incubated in 0.1% Sudan Black B for 10 min at room temperature and washed with Tx-PBS for 30 min. Sections were coverslipped with Vectashield

(Vector Laboratories) and observed with a confocal laser microscope (LSM5 PASCAL; Carl Zeiss MicroImaging GmbH, Jena, Germany).

2.6. Assessment of other pathological changes

Neurofibrillary changes and senile plaques were evaluated by the Braak stage on Gallyas–Braak and methenamine silver-stained sections, respectively. Argyrophilic grains and Lewy pathology were evaluated on Gallyas–Braak silver-stained sections and alpha-synuclein immunostained sections, respectively. TDP-43 pathology was classified into types 1–4 according to the reported pathological criteria [9].

3. Results

3.1. Clinical features of FTLD-MND-P cases (cases 1–10)

The clinical features of cases 1–10 are summarized in Table 2. The mean age of onset and disease duration were 54 years (range 48–75 years) and 12 years (range 2.7–21 years), respectively. Six of the ten cases were male. The first symptoms were FTD in the five cases, SD in three cases, PA in one case, and auditory hallucination in one case. The UMN signs were recorded in six cases, and five of the six cases developed UMN signs in the middle or late stage of the disease. The laterality of the UMN signs was recorded in four cases. The UMN signs included hyperreflexia, spasticity, Babinski's sign, paralysis, and ankle

Table 3
Antibodies used in the immunohistochemistry.

Antibody	Type	Source	Dilution
Phosphorylation-independent anti-TDP-43 TDP43C [405–414]	Rabbit polyclonal	Made by Hasegawa et al. [10]	1:1000
Phosphorylation-dependent anti-TDP-43 pS409/410	Rabbit serum	Made by Hasegawa et al. [10]	1:1000
pS403/404	Rabbit serum	Made by Hasegawa et al. [10]	1:1000
Anti-α-synuclein Pα#64	Mouse monoclonal	Wako Chemical, Osaka, Japan	1:3000
Anti-cyctatin C	Rabbit polyclonal	Dako, Glostrup, Denmark	1:3000

Table 4
Pathological features of the FTLD-MND-P cases (cases 1–10) and FTLD-MND-A cases (cases 11–16).

Case No.	Brain weight (g)	Atrophy	UMN pathology						LMN pathology			
			Neuron loss in PMC	CST degeneration					Neuron loss			
				White matter of PMC	Internal capsule	Cerebral peduncle (right/left)	Pyramid (right/left)	Spinal cord (right/left)	HN	Spinal cord	Bunina bodies	Type of TDP-43 histology
1	1350	T>F (lt)	+	-	-	-/-	3+/3+	N/N	-	N	-	3
2	1050	T=F (lt)	+	+	-	-/-	1+/1+	N/N	-	N	-	2
3	890	N	N	N	-	+/N	1+/1+	N/N	-	N	-	3
4	1060	T>F	-	-	-	-/-	1+/1+	N/N	-	N	-	1
5	1040	T>F	+	-	-	N/-	N/2+	N/N	-	N	-	1
6	690	T>F (lt)	+	-	-	+/+	3+/3+	+/+	-	-	-	3
7	915	T>F	+	+	-	+/N	N/2+	N/N	-	N	-	1
8	920	T=F	+	-	+	+/+	3+/3+	+/+ ^a	±	- ^a	-	1
9	905	T>F (lt)	±	-	-	-/+	2+/2+	+/+	-	-	-	1
10	640	T>F (lt)	+	+	N	+/N	3+/3+	+/+	-	-	-	1
11	1340	-	N	-	-	-/-	1+/1+	+/+	+	+	+	2
12	1240	T (rt)	-	-	-	-/-	-/-	+/+	+	+	+	2
13	1260	-	+	-	-	-/-	1+/1+	+/+	+	+	+	2
14	1200	T = F	+	-	-	-/-	1+/N	N/N	+	N	+	3
15	N	F > T	+	-	-	-/-	1+/1+	+/+	+	+	+	2
16	1120	T = F	-	N	-	+/N	1+/1+	+/+	+	+	+	2

N: not able to evaluate, -: absent, ±: minimal, +: present, 1+: mild, 2+: moderate, 3+: severe, T>F temporal lobe-predominant atrophy, F>T frontal lobe-predominant atrophy, T=F temporal and frontal lobes were equally atrophic. T Temporal lobe atrophy, lt left side predominant atrophy, rt right side predominant atrophy, PMC primary motor cortex, CST corticospinal tract, HN hypoglossal nucleus. ^a Only the upper cervical cord was available. The UMN pathology in the cerebrum was evaluated on the right side in cases 1, 7 and 9, and on the left side in the other cases.

clonus. There were no LMN signs in any case. In cases 2, 3, 5 and 10, there were no descriptions indicating the presence or absence of UMN signs in the medical records, and in cases 7 and 9, there was no description regarding the laterality of the UMN signs. Signs of parkinsonism such as limb rigidity and hand tremor were recorded in three cases.

3.2. Neuropathological findings of FTLD-MND-P cases (cases 1–10)

A summary of the findings in cases 1–10 is shown in Table 4. The mean brain weight was 946 g (range 640–1,350 g). Only in case 3, the cerebrum could not be evaluated macroscopically because neither brain photographs nor hemispheric sections were available. In the other cases, the frontotemporal lobes showed temporal lobe dominant atrophy in cases 1, 4–7, 9 and 10, while the frontal and temporal lobes were equally atrophic in cases 2 and 8. The laterality of frontotemporal atrophy was seen in five cases. Atrophy of the precentral gyrus was generally mild, but only case 9 showed severe atrophy on the left side. The atrophy of the pyramid of the medulla oblongata was demonstrated in cases 1 and 5–10.

Microscopically, frontotemporal cortices showed temporal lobe dominant degeneration in cases 1, 4–7, 9 and 10, whereas frontal and temporal cortices were equally degenerated in other cases. In the temporal cortex of all cases except for case 2, moderate or severe neuronal loss was observed not only in the superficial layer but also in the deep layers, and myelin loss and gliosis were demonstrated in the adjacent white matter (Figs. 1a, b, d, 3a, b). There was neither obvious LMN loss nor Bunina bodies in the hypoglossal nucleus or spinal cord in any case (Fig. 2c, e). There were no cases showing neurofibrillary changes corresponding to Braak stage III–VI. Lewy-related pathology was seen only in case 10, which showed the limbic type [26]. Argrophilic grains were not found in any case. The microscopic findings of the PMC and CST are described below.

3.2.1. PMC

The PMC was examined unilaterally in all cases except for case 3 in which the PMC could not be identified. Although the macroscopic atrophy of the left precentral gyrus was demonstrated in case 9, there were no samples from the left precentral gyrus in this case. In general, the PMC degeneration was mild when compared to other frontotemporal cortices. In detail, neuronal loss was not apparent in cases 4 and

9. In cases 2 and 5–8, mild neuronal loss and astrocytosis were demonstrated only in the superficial layer. In case 7, laminar astrocytosis was seen in the deep layers on Holzer staining. Cases 1 and 10 showed moderate neuronal loss in the superficial and deep layers (Fig. 1c). The Betz cells were sparse and showed atrophy in cases 1, 5–8 and 10. In contrast, loss of Betz cells was minimal in cases 2 and 9, and not apparent in case 4.

3.2.2. Subcortical white matter of the PMC

The subcortical white matter of the PMC was examined unilaterally in all cases except for case 3. Degeneration was demonstrated only in cases 2, 7 and 10 (Fig. 1a, b).

3.2.3. Posterior limb of the internal capsule

The posterior limb of the internal capsule was examined unilaterally in all cases except for case 10. Degeneration was demonstrated only in case 8 (Fig. 3a, b).

3.2.4. Midbrain

The cerebral peduncle was examined unilaterally in cases 3, 5, 7 and 10, and bilaterally in other cases. Degeneration was seen in the middle third of the cerebral peduncle corresponding to the CST in cases 3 and 6–10 (Figs. 2a, 3c), although cases 3, 7 and 10 showed more marked degeneration in the medial third of the cerebral peduncle corresponding to the frontopontine tract (Fig. 2a).

3.2.5. Medulla oblongata

The pyramid was examined unilaterally in cases 5 and 7, and bilaterally in other cases. Degeneration was demonstrated in all cases, and was severe in cases 1, 6, 8 and 10 (Fig. 2b), moderate (2+) in cases 5, 7 and 9, mild (1+) in other cases (Fig. 3d).

3.2.6. Spinal cord

The cervical, thoracic, and lumbar cord was available in cases 6, 9 and 10, and only upper cervical cord could be examined in case 8. The CST was involved in all cases (Fig. 2d).

3.2.7. TDP-43 pathology

Two kinds of phosphorylation-dependent antibodies against TDP-43 showed almost the same distribution and severity of abnormal structures in the brain and spinal cord. Anti-TDP43C [405–414], a

phosphorylation-independent C terminal antibody, showed abnormal structures with weak staining of normal nuclei. Six of the eight cases (cases 4, 5 and 7–10) showed type 1 TDP-43 histology in the cerebral cortex (Fig. 1e, f), three cases (cases 1, 3 and 6) type 3 histology, and one case (case 2) type 2 histology. In the cases showing type 1 histology, abundant DNPs with rare NCIs were demonstrated in the cerebral cortex, and GCIs were not observed in the gray or white matter including the CST. In the cases showing type 3 histology, abundant DNPs and NCIs were observed in the cerebral cortex, and GCIs were sparsely seen. In case 2 showing type 2 histology, abundant NCIs without DNPs were seen in the cerebral cortex, and GCIs were observed in the gray and white matter.

In all subtypes, TDP-43-positive structures were consistently observed in the frontotemporal cortices including the PMC, anterior parietal cortex, and striatum. The NCI in the Betz cell was demonstrated only in case 1. In the hypoglossal nucleus, there was no TDP-43 pathology in cases 1, 3 and 5–10, whereas only one NCI was observed in one section in case 4, and round structures in the neuropil were demonstrated in case 2. In the spinal cord anterior horn, there were rare NCIs in case 10, and rare DNPs in cases 9 and 10. In cases 9 and 10, interestingly, TDP-43-positive round structures were frequently identified in the neuropil of the anterior horn (Fig. 2f). There was no TDP-43 pathology in the spinal cord in cases 6 and 8.

3.2.8. Double labeling immunofluorescence

Double labeling immunofluorescence was performed to clarify the characteristics of the round structures in the neuropil of the spinal cord anterior horn in case 10. Confocal immunofluorescence of ubiquitin and TDP-43C [405–414] showed colocalization in an NCI, and a round structure in the neuropil (Fig. 4). Similarly, immunofluorescence of p62 and TDP-43C [405–414] demonstrated colocalization in a DN, and a round structure in the neuropil, while an NCI immunoreactive only for p62 or for TDP-43 was also seen (Fig. 4).

3.3. Clinicopathological findings of FTLD-MND-A cases (cases 11–16)

The clinicopathological findings of cases 11–16 are summarized in Table 2. The mean age of onset and disease duration were 55 years (range 39–64 years) and 3.3 years (range 1.7–6 years), respectively. Three of the six cases were male. The first symptoms were FTD in four cases, and memory impairment in two cases. Case 12 developed FTD and LMN signs simultaneously, and was given a clinical diagnosis of ALS. The longest duration of the appearance between dementia and LMN signs was six years (case 16). The UMN signs were recorded in five of the six cases, whereas the absence of the UMN signs was described in case 11. Parkinsonism was not recorded in any cases.

The mean brain weight was 1232 g (range 1120–1340 g). There was no apparent cerebral atrophy in cases 11 and 13. The frontotemporal lobes showed frontal dominant atrophy in case 15, while the frontal and temporal lobes were equally atrophic in cases 14 and 16. Case 12 showed atrophy only in the anterior temporal lobe

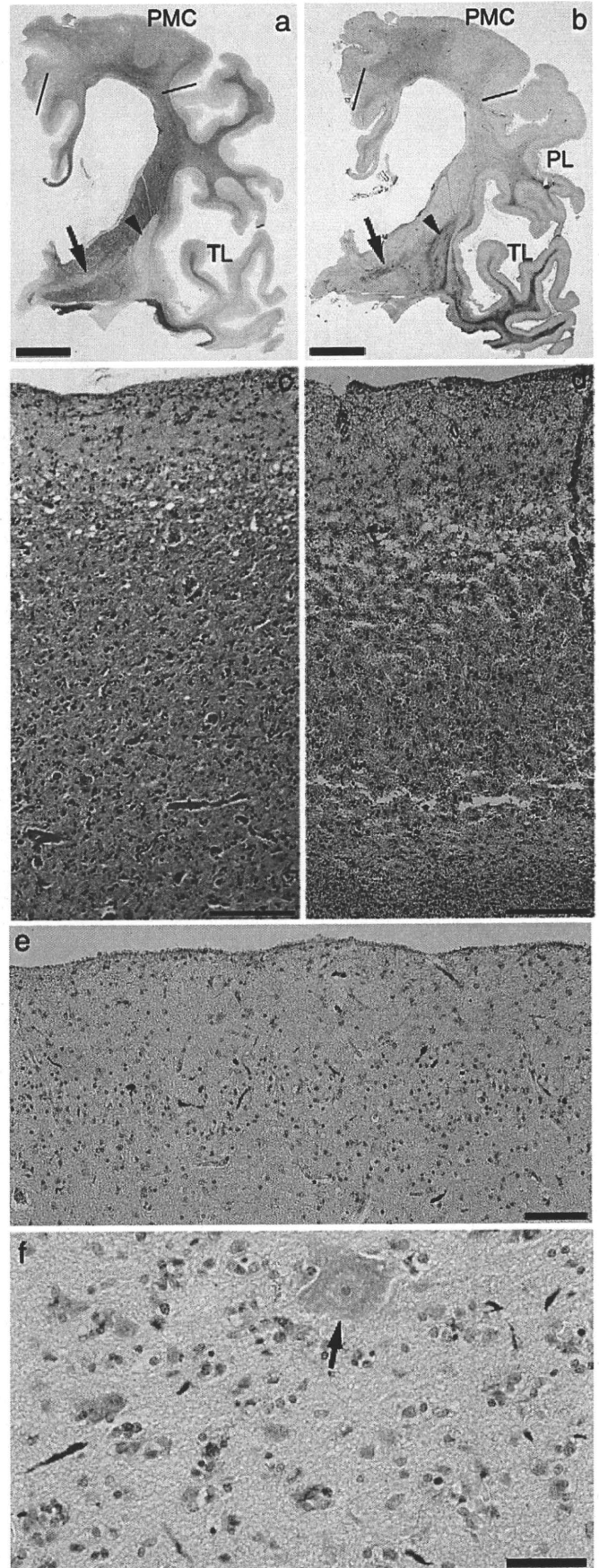


Fig. 1. (case 10) a and b are serial sections. a The left hemispheric section at the plane of the globus pallidus is shown. The area of cerebral cortex between the lines is the primary motor cortex (PMC) where Betz cells were identified. Cerebral atrophy was accentuated in the temporal lobe (TL). Enlargement of the lateral ventricle was evident, and the putamen (arrowhead) was atrophic. Mild myelin pallor was observed in the subcortical white matter of the PMC, whereas evident myelin pallor was seen in the subcortical white matter of the TL. The arrow indicates myelin pallor at the internal capsule (the anterior limb or genu). b Mild gliosis was demonstrated in the subcortical white matter of the PMC and anterior parietal lobe (PL), whereas evident gliosis was seen in the subcortical white matter of the TL. Gliosis was also seen in the internal capsule (arrow) and putamen (arrowhead). c Moderate neuronal loss was demonstrated in the superficial and deep layers of the PMC. d Severe neuronal loss was observed in the superficial and deep layers of the temporal cortex. e TDP-43 positive dystrophic neurites (DNs) were observed in the superficial layer of the PMC. f DNPs were also demonstrated in the deep layer of the PMC. The arrow indicates a Betz cell. a Klüver–Barrera stain, b Holzer stain, c, d Hematoxylin–eosin stain, e, f anti-TDP43. Scale bars a, b 1 cm, c, d 200 μ m, e 100 μ m, f 50 μ m.

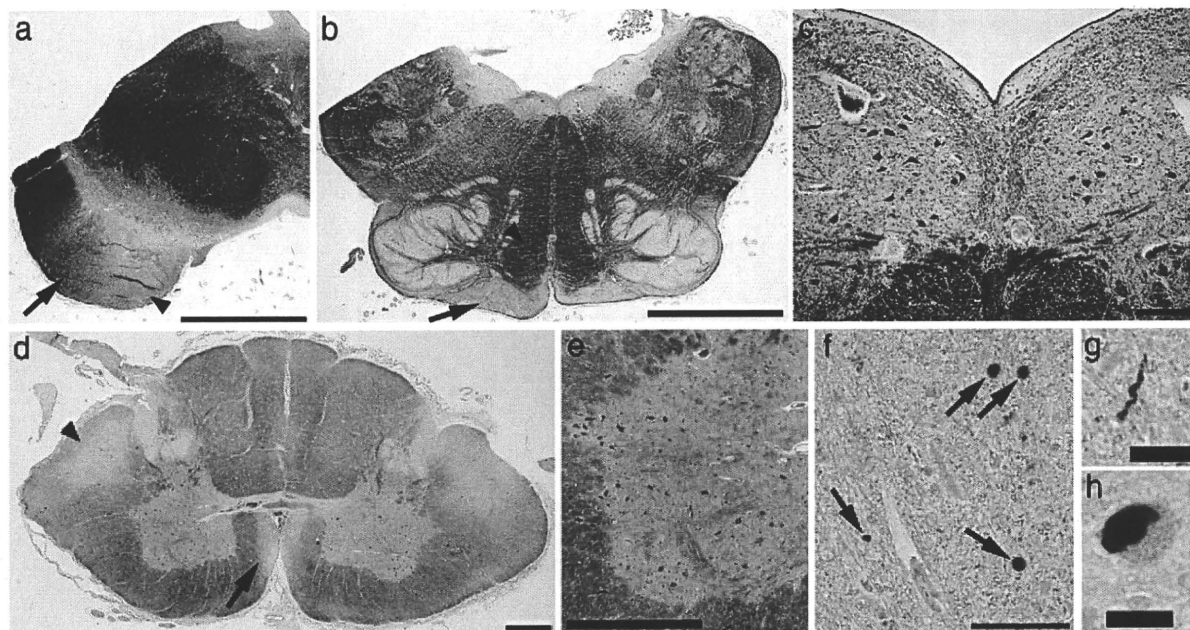


Fig. 2. (case 10) a Myelin pallor was demonstrated in the middle third of the cerebral peduncle corresponding to the corticospinal tract (CST) (arrow), although more marked degeneration was observed in the medial third of the cerebral peduncle corresponding to the frontopontine tract (arrowhead). b Atrophy and myelin pallor were demonstrated bilaterally in the pyramid of the medulla oblongata (arrow). In contrast, myelin was well preserved in the medial lemniscus (arrowhead). c Neurons were preserved in the hypoglossal nucleus. d Myelin pallor was demonstrated in the lateral (arrowhead) and anterior (arrow) CST of the cervical cord. e The cervical cord anterior horn cells were preserved. f TDP-43 positive round structures were demonstrated in the neuropil of the cervical cord anterior horn. g, h A DN (g) and a neuronal cytoplasmic inclusion (NCI) (h) were observed in the cervical cord anterior horn. a–e Klüver–Barrera stain, f–h anti-TDP43. Scale bars a, b 5 mm, c 200 μ m, d, e 1 mm, f 50 μ m, g, h 20 μ m.

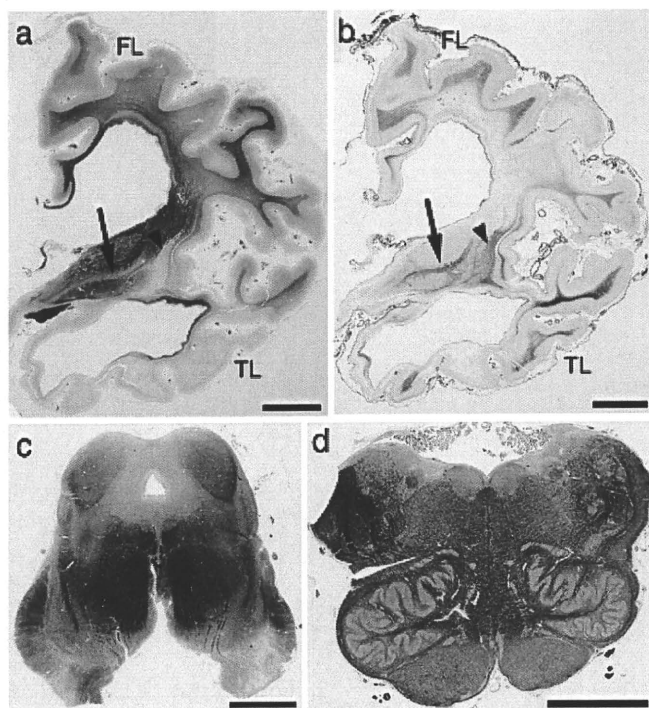


Fig. 3. a and b are serial sections of case 8. a The left hemispheric section at the plane of the posterior limb of the internal capsule showed the atrophy of the frontal lobe (FL), temporal lobe (TL) and putamen (arrowhead). The lateral ventricle was markedly enlarged. Myelin pallor was demonstrated in the posterior limb of the internal capsule (arrow), and white matter of the FL and TL. Betz cells were not identified in this section. b Gliosis was observed in the posterior limb of the internal capsule (arrow), putamen (arrowhead), and white matter of the FL and TL. c Myelin pallor was evident in the middle third of cerebral peduncle in case 6. d Myelin pallor without atrophy was observed bilaterally in the pyramid of the medulla oblongata in case 4. a, c, d Klüver–Barrera stain, b Holzer stain. Scale bars a, b 1 cm, c, d 5 mm.

predominantly on the right side. In case 11, the degree of the degeneration of the cerebrum could not be evaluated microscopically because there were severe hypoxic changes throughout the cerebrum. In all other cases, neuronal loss and gliosis in the frontotemporal cortices were noted only where macroscopic atrophy was demonstrated. In the PMC, neuronal loss in the superficial layer was demonstrated only in case 13, while Betz cells were sparse and showed atrophy in cases 13–15. The CST was involved in the spinal cord in all five cases in which the spinal cord could be examined. Degeneration of the pyramid of the medulla oblongata was limited to show myelin pallor without atrophy (mild, 1+) in cases 11 and 13–16, and was not apparent in case 12. The CST was spared in the cerebral peduncle in cases 11–15. In all cases, the CST was involved neither in the internal capsule nor subcortical white matter of the PMC, although the subcortical white matter of the PMC could not be evaluated in case 16 because diffuse leukoaraiosis related to the hyalinosis of the vessel walls was present. There were evident LMN loss and Bunina bodies in the hypoglossal nucleus and spinal cord in all cases.

TDP-43 immunohistochemistry showed type 2 histology in five of the six cases (cases 11–13, 15 and 16), and type 3 histology in case 14, in which a small number of NIs was demonstrated in the frontal cortex. In the PMC, NCIs were seen in cases 11 and 14, although the PMC of cases 13 and 15 could not be evaluated by immunohistochemistry. There were no NCIs in the Betz cells in any case. In all six cases, NCIs were demonstrated in the LMNs of the brainstem and/or spinal cord, and GCIs were variably seen in the gray and white matter including the CST. In the spinal cord anterior horn, GCIs were demonstrated in cases 11 and 15, and DNs were seen in case 11. Only in case 13, TDP-43-positive round structures were observed in the neuropil of the anterior horn.

3.4. Comparison between FTLD-MND-P and FTLD-MND-A cases

Comparison of the clinicopathological findings between FTLD-MND-P and FTLD-MND-A is shown in Table 5. The mean disease duration of

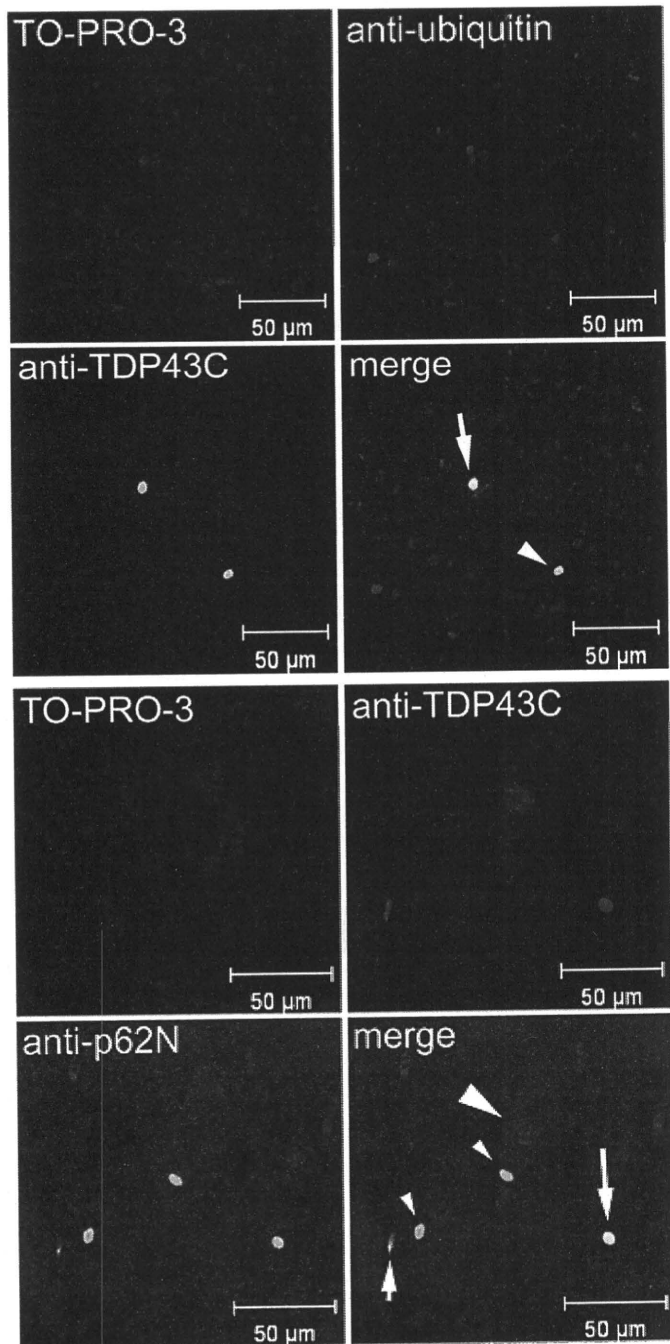


Fig. 4. The cervical cord anterior horn of case 10 was investigated. Nuclei were stained with TO-PRO-3 (Invitrogen, Tokyo, Japan), producing a blue color. Confocal immunofluorescence of ubiquitin and TDP-43C [405–414] showed colocalization in an NCI (arrow) and a round structure in the neuropil (arrowhead). Confocal immunofluorescence of TDP-43C [405–414] and p62N demonstrated colocalization in a DN (short arrow) and a round structure in the neuropil (long arrow). The small arrowheads show NCIs immunoreactive only for p62N, and the large arrowhead an NCI immunoreactive for only TDP-43.

FTLD-MND-P (12 years) was much longer than that of FTLD-MND-A (3.3 years). The CST degeneration was severe in FTLD-MND-P cases, for instance, the pyramid of the medulla oblongata showed atrophy in seven of the ten FTLD-MND-P cases while FTLD-MND-A cases did not show atrophy of the pyramid. In addition, CST degeneration was seen in the cerebral peduncle in six of the ten FTLD-MND-P cases, whereas it was demonstrated only in one of the six FTLD-MND-A cases. Small brain weight and severe CST degeneration in FTLD-MND-P cases may be partly explained by the prolonged disease duration.

4. Discussion

In our FTLD-MND-P cases, UMN signs were observed in six of ten cases, whereas LMN signs were not seen in any case. The relatively prolonged disease duration of FTLD-MND-P cases may be related to the lack of LMN signs. Histopathologically, there was no obvious LMN loss or Bunina bodies in any case. These clinical and histopathological findings are distinct from those of FTLD-MND-A. Considering the type of TDP-43 histology in the cerebral cortex, however, type 2 or 3 histology was demonstrated in the cerebral cortex of some FTLD-MND-P cases; therefore, it may be difficult to exclude the possibility that these FTLD-MND-P cases are actually an atypical form of FTLD-MND-A. The limitation of this study is that the spinal cord tissue was not available from six of ten FTLD-MND-P cases. In our institution, however, there were no FTLD-MND-A cases showing spinal cord anterior horn degeneration without hypoglossal nucleus involvement, and this finding in FTLD-MND-A has also been described by other investigators [27]. The spinal cord anterior horn should be fully examined in a larger number of FTLD-TDP cases in the future study.

Among the 29 FTLD-TDP cases examined in our institution, the LMNs were involved in all cases showing type 2 histology except for one case (case 2), whereas they were involved only in one (case 14) of the cases showing type 3 histology and never affected in cases showing type 1 histology. Based on this finding, the increases in disease duration from type 2 to 3, and to 1 may be explained by the degree of LMN involvement in each subtype.

The CST is involved in various brain diseases such as cerebrovascular diseases or degenerative diseases, and the latter is not limited to MND [17–19,28–32]. In contrast to the cerebrovascular diseases, CST degeneration in the degenerative diseases is often more severe at lower than at higher levels, and is thought to arise from axonopathy with peripheral “dying back” [29,33,34]. As a result of slow and gradual involvement of the motor cortex in degenerative diseases, the axon most distant from the motor cortex may be first affected. In our FTLD-MND-P cases, the CST was involved in the spinal cord and medulla oblongata in all cases in which these structures could be examined, but the CST in the midbrain, internal capsule, and subcortical white matter of the PMC was spared in some cases. CST degeneration in FTLD-MND-P appeared to be related to peripheral dying back as seen in other degenerative diseases.

To date, cases of FTLD with ubiquitin-positive, tau-negative inclusions (previously called as FTLD-U) showing CST degeneration but lacking both LMN loss and Bunina bodies have been reported not only from our institution but from other institution in Japan [28,31]. The disease duration of these two cases was 9 years [28] and 11 years [31], respectively. TDP-43 immunohistochemistry is needed to determine whether these cases are FTLD-TDP.

In this study, we showed for the first time the accumulation of TDP-43 in the spinal cord of cases showing type 1 histology, which also showed colocalization with ubiquitin and p62. Interestingly, this TDP-43 rarely accumulated in the cytoplasm of neurons as seen in the cerebral cortex showing type 1 histology, and manifested as round structures in the neuropil of the anterior horn. We speculate that one part of the DNs is not seen because these round structures are more frequently observed than typical vermiform DNs. The morphology suggested swollen processes like spheroids, but the site of accumulation is unclear at present. Since LMN loss was not apparent in the spinal cord of cases showing type 1 histology, these round structures do not appear to result in neuronal loss in the anterior horn.

In conclusion, our FTLD-MND-P cases showed characteristic clinicopathological features distinct from those of FTLD-MND-A. Type 1 of TDP-43 histology in FTLD-MND-P cases suggests that the underlying disease process differs from that of FTLD-MND-A, while cases showing type 2 or 3 histology might be the atypical form of FTLD-MND-A.